PHYSICAL REVIEW A VOLUME 1, NUMBER 3 MARCH 1970

Differential and Integral Cross Sections for Excitation of the 2^1P State of Helium by Electron Impact

Donald G. Truhlar, James K. Rice, and Aron Kuppermann
Arthur Amos Noyes Laboratory of Chemical Physics, [*]
California Institute of Technology, 1201 *East California Boulevard*, *Pasadena*, *California* 91109

and

S. Trajmar
Physics Section, [†] *Jet Propulsion Laboratory*,
California Institute of Technology, 4800 *Oak Grove Drive*, *Pasadena*, *California* 91103

and

D. C. Cartwright [‡]
Institute for Extraterrestrial Physics, *The Max Planck Institute for Physics and Astrophysics*, *Munich*, *Germany*
(Received 16 June 1969; revised manuscript received 31 October 1969)

Differential scattering cross sections for excitation of helium by electron impact from its ground state to its 2^1P excited state have been measured at four incident electron energies in the range 26–55.5 eV for scattering angles between 10° and 70°, and at 81.6 eV for scattering angles between 10° and 80°. These differential cross sections have been placed on an absolute scale by normalizing them to the experimental absolute integral cross sections of Jobe and St. John. These experimental differential and integral cross sections have been compared with the results predicted by the Born approximation, and by several other first-order approximations in which direct excitation is calculated in the Born approximation and exchange scattering by various Ochkurlike approximations. The calculations provide reliable tests of these scattering theories since they are made using the accurate generalized oscillator strengths of Kim and Inokuti. As expected, these first-order theories are poor near threshold and exchange is important at high scattering angles for all energies. Further, the absolute magnitude of the calculated integral and small-angle differential cross sections is too large and is within 50% of experiment only at energies greater than 80 eV. These first-order models are in qualitative agreement with the experimental angular dependence at 34–81.6 eV for scattering angles between 10° and 40°. At higher scattering angles (corresponding to momentum transfers greater than about 1.6 a.u.), the calculated differential cross sections fall well below the experimental ones. The phase between the direct and exchange scattering amplitudes was found to be important at all energies, and is apparently not predicted correctly by any of the first-order models examined here. Some approximations for the exchange (e.g., Ochkur approximation and the post interaction form of the Ochkur-Rudge approximation) were found to be better for integral cross sections and some (e.g., prior Ochkur-Rudge approximation) were better for differential cross sections. The use of good analytic self-consistent-field (SCF) wave functions for both the ground and excited states was tested by computing generalized oscillator strengths from them and comparing these results with the calculations using the accurate generalized oscillator strengths. The SCF functions yield differential cross sections in quantitative disagreement (20%) with the accurate results, although the energy and angle dependence of the cross sections is predicted qualitatively correctly.

I. INTRODUCTION

This paper presents a theoretical and experimental study of the differential cross section for excitation of helium from the $1s^2\,1^1S$ ground state to the $1s2p\,2^1P$ excited state by electron impact. We are concerned only with energies in the nonresonance regions. Another article[1] uses the same methods to study excitation to the 2^1S state.

The excitation energy ΔE of the 2^1P state of He is 21.22 eV. Because of the close proximity of the 2^3P state ($\Delta E = 20.96$ eV), a high resolution apparatus is required to determine the differential cross section for excitation of the 2^1P state at electron-impact energies E below about 100 eV. (At higher energies, the excitation of the 2^3P becomes less likely[2] for at least some angles, and then the closest peak is the 2^1S at 20.61 eV.) Six previous high-resolution measurements of the 2^1P differential cross section [3–8] are summarized in Table I.

TABLE I. Measurements of the differential cross section for the $1^1S \rightarrow 2^1P$ transition is helium.

Reference	E (eV)	θ (deg)
3	417–604	3.8 – 12
4	500	6.3 – 15.3
5[a]	56.5	5 – 70
6	400	1.5 – 4.0
7	100–400	5 – 20
8	21–23	10 – 145
10[b]	34	10 – 70
This paper [b]	26.5–81.6	10 – 80

[a]The 2^3P excitation was present but not clearly resolved in these measurements.
[b]Present experiments.

(Some of the older data is discussed in Ref. 1.) The table shows that prior to the present work little was known about the energy and angle dependence of the differential cross section, except for high energies and/or scattered angles (θ) less than 20°. In fact, the differential cross section was known over an angular range $\Delta\theta > 15°$ at only one energy much above threshold. The determination of large angle differential cross sections requires a very sensitive detection system so that low enough pressures to avoid double scattering difficulties[9] can be used. In this research we used our high-resolution variable-angle electron-impact spectrometer[10] to obtain the differential cross section for $10° \leq \theta \leq 80°$ at five energies. The 2^3P excitation is completely resolved from the 2^1P in all the spectra reported here. The energy and angle range of the present experimental investigation are included in Table I for comparison. By using the experimental 2^1P integral cross sections of Jobe and St. John,[2] we are able to put our experimental differential cross sections on an "absolute" basis.

As has been demonstrated previously,[10–12] electron-impact spectra for intermediate incident energy and large angular range are very useful for the discovery and elucidation of molecular excited states, particularly those whose excitation by photon impact is forbidden. Also, as will be shown below, such experimental data provides a stern test for any approximate theory. For these reasons we make an extensive theoretical analysis of our results in an attempt to ascertain upon what foundation our interpretation of such spectra can rest. We analyze the low-energy variable-angle data to see in what way it can and cannot be related to a first-order mechanism which includes both direct excitation by means of the Born approximation[13,14] and also exchange excitation through various Ochkur-Bonham-like relations,[15,16] some of which have not previously been tested. By using recent and very accurate generalized oscillator strengths, calculated from correlated wave functions by others,[17–19] we can confidently test the various approximations. Also, by calculating the corresponding generalized oscillator strengths using self-consistent-field (SCF) wave functions, we can test how the predictions are modified using accurate wave functions of the type usually available for molecules. (After the present work was well under way, Kim and Inokuti[19] suggested another reason why a calculation, such as ours, using accurate Hartree-Fock wave functions would be of interest. We discuss this in Sec. III D.) Another important motivation for performing these calculations is that the Born approximation with Ochkurlike corrections for exchange is calculated by evaluating the expectation for a one-electron transition operator – a calculation which is practical even for large scattering systems. The theoretical considerations are extended to cover not only our new data but also some of the other data referred to in Table I.

Recently, much interest has been focused on determining the applicability of the Born approximation and various generalized Born approximations.[20–29] Several investigations of electron excitation of helium to the 2^1P and 3^1P states are particularly pertinent here. Silverman and Lassettre[24] used a semiempirical technique to show that the Born approximation does not give an integral cross-section curve which agrees with the experiments of St. John, *et al.*[30] for the excitation of the 3^1P state below about 100 eV. Vriens, *et al.*[7] showed by similar technique that there were small departures from the Born-approximation prediction for the small-angle differential cross section for 2^1P excitation at energies below 200 eV, but that the theory was qualitatively correct down to 100 eV, the lowest energy they considered. Kennedy and Kingston[17] used accurately calculated generalized oscillator strengths to test the 2^1P integral cross section and found good agreement of the Born approximation with the experiments of Moustafa Moussa and de Heer[31] at energies down to 50 eV. The accurate Born calculations of Kim and Inokuti[19] and the recent experiments of Jobe and St. John[2] agree with the cross sections used for the comparison mentioned in the last sentence; however, Kim and Inokuti found that the small-angle differential cross section is represented quantitatively by the Born approximation only at and above 200 eV. Bell, *et al.*[18] calculated generalized oscillator strengths for the 3^1P state and found agreement with experimental integral cross sections[31] down to about 100 eV, confirming the result of Silverman and Lassettre.[24] For this state, they also studied the effect on the integral cross section of including exchange by the prior Ochkur and prior Ochkur-Rudge (OR) approximation. These corrections extended the range of agreement of theoretical and experimental integral cross sections only slightly. In the present re-

search, we are interested both in the accuracy of predicted integral cross sections over the whole energy range and also of the predicted behavior of the differential cross sections over a wide angular range at low and intermediate energies.

II. EXPERIMENTS

A. Apparatus

The low-energy variable-angle electron-impact spectrometer used in these experiments is shown schematically in Fig. 1. It consists of an electron gun, two hemispherical electrostatic energy analyzers (for generating a monochromatic electron beam and energy analyzing, i.e., selecting, the scattered electrons), a flexible welded-bellows scattering chamber, and an electron-multiplier detector. Details of the spectrometer's construction and operation can be found elsewhere.[11]

B. Experimental Procedure

High-purity dry helium was admitted to the scattering chamber at a rate which provided a constant pressure (within 5%) of $1-3\times10^{-3}$ Torr, as measured by an uncalibrated ion gage. The instrument was tuned to a resolution of about 0.10 eV (full width at half-maximum of the elastic peak) for a fixed incident energy and an incident beam current of about 5×10^{-8} A. This resolution is sufficient to clearly separate transitions to the 2^1P level from those to the 2^3P one, which lies closest in energy loss. It is evident from earlier work[32] that a failure to resolve these two features can lead to erroneous results at large scattering angles and low incident energies.

The zeros of the energy loss and scattering-angle scales were defined in terms of the elastically scattered electrons. In addition, the intensity distribution of inelastically scattered electrons ($1^1S \rightarrow 2^1P$)

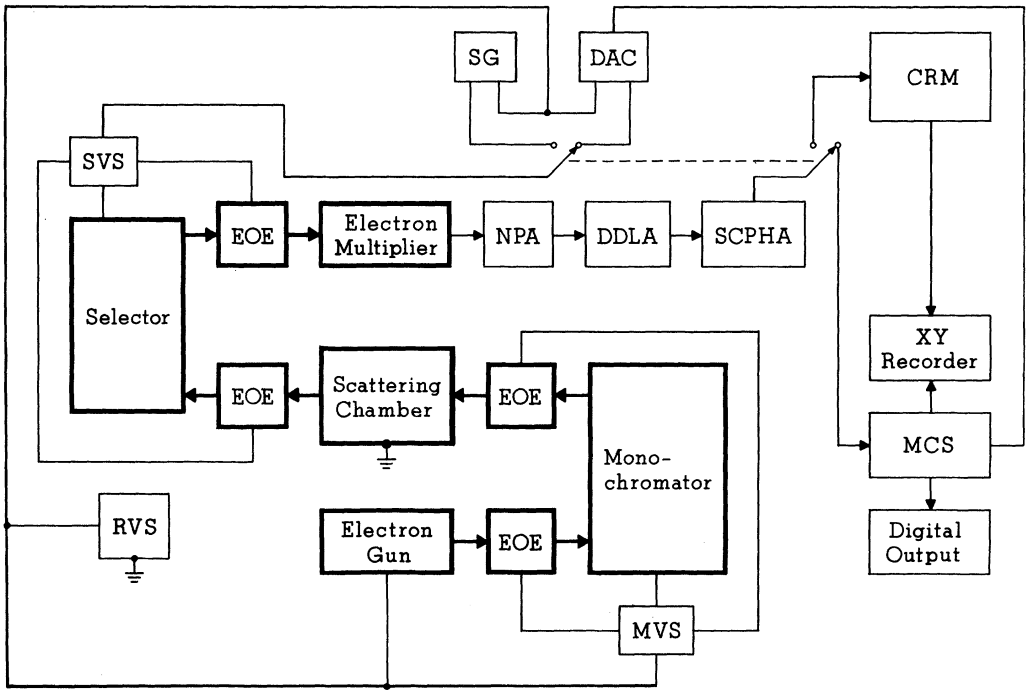

FIG. 1. Schematic diagram of the electron-impact spectrometer. The kinetic energy of the electron beam at the scattering chamber is determined by the reference voltage supply (RVS). Appropriate voltages are applied to the monochromator, selector, and their associated electron optical elements (EOE) by the monochromator and selector voltage supplies (MVS and SVS, respectively). Scattered electrons which reach the electron multiplier produce pulses which are preamplified by a nuvistor preamplifier (NPA), amplified by a double-delay-line amplifier (DDLA), and then discriminate by a single-channel pulse-height analyzer (SCPHA) to eliminate low-level electrical noise. The output of the SCPHA can be routed to a 1024-channel scalar (MCS) or a count-rate meter (CRM). In the former case, the voltage used to sweep the energy loss spectrum is supplied by a digital-to-analog converter (DAC) that converts the number of the channel into which counts are being stored to an analog signal specifying the energy loss. In the latter case, the voltage sweep is supplied by a sweep generator (SG). The output of the MCS (e.g., counts/channel) can be recorded digitally on punched paper tape, displayed visually on an oscilloscope (not shown in figure), or plotted continuously on an X-Y recorder. The signal from the CRM can be plotted on the X-Y recorder. The scattering angle is variable.

was measured in several cases to $-20°$ and found to be symmetric about $\theta = 0°$, as defined above. The incident energy was calibrated in each experiment by observation of the 57.1- and 58.2-eV helium resonances[5] and taking the correction so determined to be independent of incident energy. This calibration was done for all experiments except those at 81.6 eV, for which no calibration was made. This calibration required a change of 1 eV or less from the nominal incident energy, as set by the instrument power supplies. Thus, we believe the quoted impact energies to be accurate within about 1 eV.

The basic experimental measurements consist of the determination of the intensity of electrons scattered after losing an energy corresponding to excitation of the 2^1P state. This determination was made by scanning the 2^1P energy-loss feature and measuring its peak intensity with a count-rate meter as a function of scattering angle for fixed incident energies of 26, 34, 44, and 55.5 eV. Each peak intensity was normalized to the same incident beam current. Our use of peak heights rather than areas is justified by the fact that the peak shapes do do not change with angle.

Since the intensities at each scattering angle correspond to a different scattering geometry, they have been normalized to the same geometry (in order to obtain 2^1P differential cross sections in arbitrary units) by a procedure previously discussed.[11] (The preliminary results in Ref. 10 were normalized by a simplified procedure.) The normalization assumes at each angle that the differential cross section is constant over the range of scattering angles (about $\pm 2\frac{1}{2}°$) that actually contribute to the intensity at any one nominal scattering angle [the range would be negligibly small if the beam and view cones were narrow rays (see Ref. 11)].

At 81.6 eV, the intensity of inelastically scattered electrons had become so low that long data collection times were required (from 1–24 h, typically 10, at a single angle). Thus, it was possible that the instrumental conditions for data collection at one scattering angle might not have been identical to those for another angle. To circumvent this problem, the energy-loss spectrum at each angle was obtained by first scanning the elastic peak, then jumping in energy loss to 18.95 eV, which is below the first inelastic feature at 19.82 eV (2^3S), and then scanning to 21.35 eV. This process was repeated from about three times at smaller angles to as many as 162 times at larger ones using a multichannel scaler[11] to accumulate the result of each scan, thereby increasing the signal-to-noise ratio of the 2^1P feature. The ratio of the 2^1P peak height to that of the elastic one was determined at each scattering angle from the result. An example of such an accumulated energy-loss spectrum is given in Fig. 2. Subsequently, separate determinations of the elastic differential

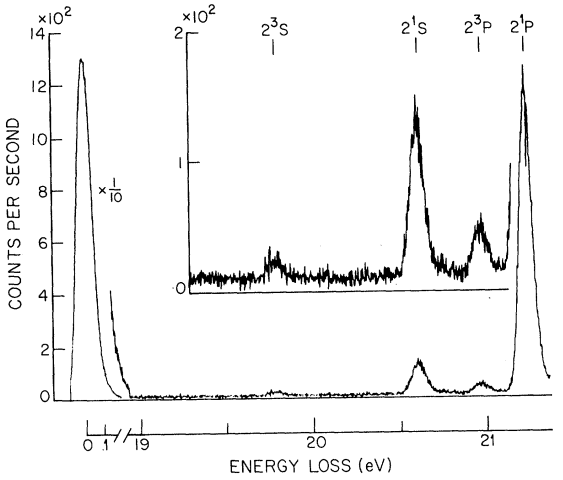

FIG. 2. Energy-loss spectrum of helium at $E = 81.6$ eV and $\theta = 22°$. The elastic peak, which defines the zero of energy loss, has been reduced by a factor of 10 before plotting. This spectrum was obtained by accumulating the results of five consecutive scans in the 1024 channels of the multichannel scalar. Dwell time per channel = 1 sec; time per scan = 17 min; scan rate = 0.0026 V/sec; helium pressure = 1.5×10^{-3} Torr; incident beam current = 6.4×10^{-8} A. We obtained the ordinate in counts per seconds by dividing the measured counts per channel by five. The insert displays the same data with an expanded ordinate scale.

cross section were made during the periods that were short (about 2 h) compared to that associated with instrumental instabilities. In addition, during this determination we verified that the instrumental conditions did not change. Finally, multiplication of the 2^1P elastic ratios by this elastic differential cross section yielded the 2^1P differential cross section (in arbitrary units).

The error bars assigned to the experimental differential cross sections were determined from the reproducibility of the peak-intensity data (average deviation of three to five values at each angle) or the ratio data in the 81.6-eV case and from the uncertainty in the scattering geometry normalization. The errors average 15% for $E = 26$–55.5 eV and 37% at 81.6 eV. The possibility that these measurements were affected by double scattering[9] has been eliminated by verifying that the scattered signal was linear with pressure up to 5×10^{-3} Torr at several angles for each impact energy.

The absolute scale for the differential cross sections was determined in the following manner. The DCS $I(\theta)$ is related to the integral cross section Q by

$$Q(E) = 2\pi \int_0^\pi I(E, \theta) \sin\theta \, d\theta. \tag{1}$$

If the experimental differential cross section were

known from 0° to 180° at each energy, we could integrate it and use the experimental $Q(E)$ of St. John and Jobe[2] to put it on an absolute scale. We carried out this procedure, but since our differential cross section is not known over the full 180°, we had to estimate its value at $\theta < 10°$ and $\theta > 70°$ (or $\theta > 80°$ at 81.6 eV). This estimation is particularly simple for the 2^1P state because of the smooth monotonic nature of the differential cross section in the 30°–70° range. The uncertainty of the differential cross section below 10° does not introduce much error in the integral (1) because of the $\sin\theta$ weighting factor. Because the small phase shifts in the higher partial waves determine the shape of the low-angle scattering, this shape can be well predicted by using the first-order calculations described below. These calculations predict that the differential cross section flattens out in the region of small scattering angles. To extrapolate the experimental data, we assumed the differential cross section is linearly increasing for $\theta \leq 10°$ with a slope determined by the lowest angle points. A change in this slope by a factor of 2 from that which we used only changes the value of the 0°–70° integral by 2–4%. Using an exponential extrapolation instead of a linear one for this purpose changes the results less than 1%. Except at 81.6 eV, the uncertainty in the integral (1) over the range 0–80° is probably about 15%, since this is the approximate relative error in each experimental point $I(E, \theta)$. At 81.6 eV this error is about 35%. The data were extrapolated to 180° by assuming

$$I(E, \theta) = A_E\, q^{-N_E}, \tag{2}$$

where A_E and N_E were determined from $I(E, 60°)$ and $I(E, 70°)$, and $q(\theta)$ is the magnitude of the momentum transfer. The breakdown of the integral (1) into regions 0°–70° and 70°–180° for the differential cross section normalized this way is given in Table II. Also included is an estimate of the percent error which is based on consideration of both regions of the integral. This is probably an upper limit, since the error for the second range is taken as that which would occur if the correct $I(E, \theta)$ were a constant for $70° \leq \theta \leq 180°$ (or $80° \leq \theta \leq 180°$ in the 81.6-eV case).

C. Results

The 2^1P differential cross section $[I(E, \theta)]$ was determined for $10° \leq \theta \leq 70°$ at energies of 26, 34, 44, and 55.5 eV, and for $10° \leq \theta \leq 80°$ at 81.6 eV. For reasons discussed elsewhere,[1] the lowest energy point will be considered to be at 26.5 eV. These five differential cross sections are given in Figs. 3–7 (note that for purposes of display the experimental results are multiplied by the scale factors given in the captions). The theoretical curves in these figures will be discussed in Sec. V. An interesting aspect of the experimental results is that the shape of the differential cross section is the same within experimental error at impact energies of 44 and 55.5 eV.

The differential cross section at 55.5 eV can be compared in shape with that of Simpson, Menendez, and Mielczarek (SMM)[5] at 56.5 eV. The agreement is excellent for $\theta \leq 25°$, but the SMM data is probably in error due to double scattering[9] at higher angles. However, the good agreement at the smaller angles indicates that our volume correction is probably accurate to within the errors of SMM (unknown) and the present work (about 14%).

III. THEORY

A. Notation

We shall use the following notations: $\vec{r}$ is the vector to the sth electron from the He nucleus (taken as c.m.); $\vec{k}_0$, $\vec{k}_n$ are the wave-number vectors of the incident and scattered electrons, respectively. $\vec{k}_i = m\vec{v}_i/\hbar$; m is the mass of the electron; $\vec{v}_i$ is the velocity of the scattering electron; E_i is the energy of the atom in state i; and E_T is the total energy $E_T = E_i + (\hbar^2/2m)k_i^2$. Ψ_i is the spatial electronic wave function of the atom in state i; U_i is the ionization potential of the atom in state i; $\theta = \arccos(\hat{k}_0 \cdot \hat{k}_n)$ and $\vec{q} = \vec{k}_0 - \vec{k}_n$. The momentum transfer is $\hbar\vec{q}$. f is the direct scattering amplitude, and g is the exchange scattering amplitude.

In the following, we shall use hartree a.u.[33]

TABLE II. Integration and normalization of the 2^1P integral cross sections $Q(a_0^2)$.

E (eV)	Range	Contribution to Q	Range	Contribution to Q	Q	EPE [a]
26.5	0–70°	0.0468	70–180°	0.0032	0.050	38
34	0–70°	0.121	70–180°	0.013	0.134	22
44	0–70°	0.199	70–180°	0.029	0.228	22
55.5	0–70°	0.241	70–180°	0.041	0.282	21
81.6	0–80°	0.320	80–180°	0.002	0.322	37

[a] Estimated percent error.

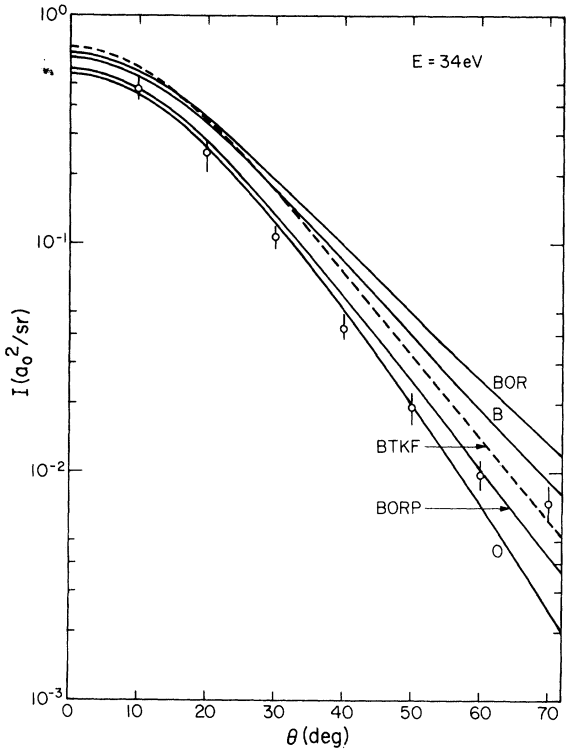

FIG. 3. Theoretical (lines) and experimental (circles with error bars) differential cross sections for excitation of the 2^1P state of helium at $E=34$ eV. The solid lines are theoretical differential cross sections calculated from the Kim-Inokuti (KI) set of ϕ_{0n}. The labels on the curves are summarized in footnote b of Table X. The Born-transferred VPS approximation (not shown) is the same as the O within plotting accuracy. For clarity of presentation, the symmetrized BOR approximation, which would lie entirely between the O and BORP is not shown. The BTKF crosses the BOR from above at 18° and the B from above at 28°. The experimental cross section is here arbitrarily normalized to the post BOR approximation at 10° by multiplying it by 2.37.

B. Methods

The integral (Q_{0n}) and differential (I_{0n}) cross sections for excitation of an excited singlet state n of the helium atom from the ground state 0 are related by Eq. (1), where

$$I_{0n}(\theta) = (k_n/k_0)\,|A_{0n}|^2 \ , \tag{3}$$

and $A_{0n}=f-g$. In the Born approximation $f=f^{\mathrm{B}}$ and $g=0$, where[34-36]

$$f^{\mathrm{B}} = -\frac{1}{2\pi}\iiint e^{i(\vec{k}_0-\vec{k}_n)\cdot\vec{r}_3}\Psi_n^*(\vec{r}_1,\vec{r}_2)\Psi_0(\vec{r}_1,\vec{r}_2) \times\left(\frac{1}{r_{31}}+\frac{1}{r_{32}}\right)d\vec{r}_1 d\vec{r}_2 d\vec{r}_3 \ , \tag{4}$$

$$f^{\mathrm{B}} = \frac{1}{2\pi}\iiint e^{i(\vec{k}_0-\vec{k}_n)\cdot\vec{r}_3}\psi_n^*(\vec{r}_1,\vec{r}_2)\Psi_0(\vec{r}_1,\vec{r}_2)$$

$$= -(2/q^2)\mathcal{E}_{0n} \ , \tag{5}$$

$$\mathcal{E}_{0n} = 2M \ , \tag{6}$$

and

$$M = \int \Psi_n^*(\vec{r}_1,\vec{r}_2)\,e^{i\vec{q}\cdot\vec{r}_1}\Psi_0(\vec{r}_1,\vec{r}_2)\,d\vec{r}_1 d\vec{r}_2 . \tag{7}$$

Equation (7) is written in the length formulation of the integral.[37] There is no post-prior discrepancy in the Born approximation.

In the Born-Oppenheimer (BO) scattering approximation,[38] $f=f^{\mathrm{B}}$ and $g=g^{\mathrm{BO}}$, where [34, 35]

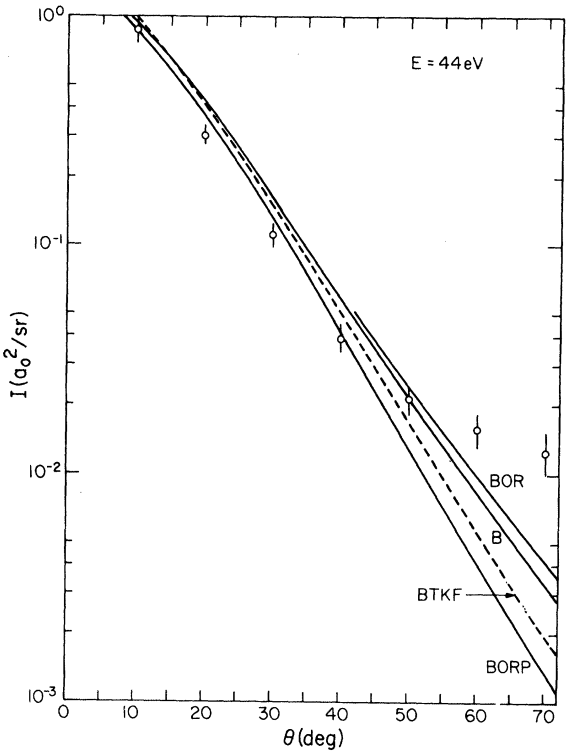

FIG. 4. Theoretical (lines) and experimental (circles) differential cross sections for excitation of the 2^1P state of helium at $E=44$ eV. The theoretical DCS's are calculated from the KI set of ϕ_{0n}. The BOR is not plotted below 42°, where it is within 6% of B. The BTKF differential cross section crosses the BOR at 19° and the B at 21°. The experimental cross sections (Sec. II C) were multiplied by 2.17 so as to show the difference in shapes of the experimental and theoretical differential cross sections.

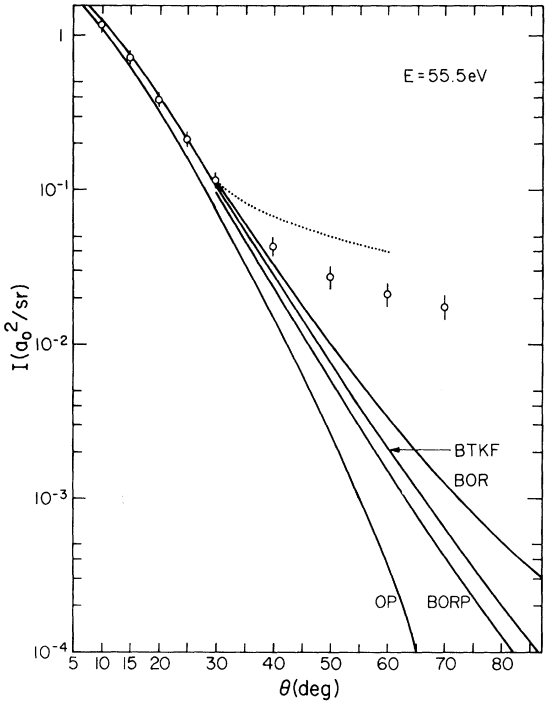

FIG. 5. Experimental and theoretical differential cross sections for excitation of the 2^1P states of helium at $E=55.5$ eV. The circles with error bars are the present experimental results multiplied by 2.27. The experimental results of Simpson *et al.* (Ref. 5) at $E=56.5$ eV agree with the present results for $\theta \leq 30°$ and are given by the dotted line at larger angles. The theoretical differential cross-section curves are calculated from the KI set of ϕ_{0n}. The Born approximation is not shown because it is within 3% of the BOR up to 60° and is $8\frac{1}{2}$% below it at 70°. The OP is shown because it is in worst agreement with experiment (it has a zero around 70°); the others because they are in best agreement of all the theories we considered. For clarity of presentation, the BOR and BORP are not shown below 30°, where all these cross sections are similar.

$$g^{\mathrm{BO}} = -\frac{1}{2\pi}\int\int\int e^{i\vec{k}_0\cdot\vec{r}_3 - i\vec{k}_n\cdot\vec{r}_1}\,\Psi_n^*(\vec{r}_3,\vec{r}_2) \times\Psi_0(\vec{r}_1,\vec{r}_2)\left(\frac{1}{r_{31}}+\frac{1}{r_{32}}-\frac{2}{r_3}\right)d\vec{r}_1\,d\vec{r}_2\,d\vec{r}_3. \quad (8)$$

In the Ochkur modification of this amplitude, $g=g^{\mathrm{O}}$, where[15,39]

$$g^{\mathrm{O}} = -(2/k_0^2)M. \quad (9)$$

Only the first of the three terms in the interaction potential (8) contributes to (9). It is convenient to introduce the generalized oscillator strength defined by [14,40,41]

$$\phi_{0n}(q) = (2/q^2)\,(E_n - E_0)\,|\mathcal{S}_{0n}(q)|^2\ . \quad (10)$$

Within the framework of perturbation theory, the differential cross section can be expressed as

$$I_{0n}(\theta) = (k_n/2k_0\,\Delta E)\,|B|^2 q^2 \phi_{0n}(q), \quad (11)$$

where $\Delta E \equiv E_n - E_0$ and

$$|B|^2 = |-(2/q^2) - G|^2 = (4/q^4) + |G|^2 + (4/q^2)\,\mathrm{Re}G. \quad (12)$$

G is a quantity defined differently in the different theories discussed below. The integral cross section can now be obtained in terms of the generalized oscillator strength from (1) and (11) or from [28]

$$q_{0n} = \frac{\pi}{k_0^2(E_n - E_0)}\int_{q_{\min}}^{q_{\max}} |B|^2\,\phi_{0n}(q)q^3\,dq, \quad (13)$$

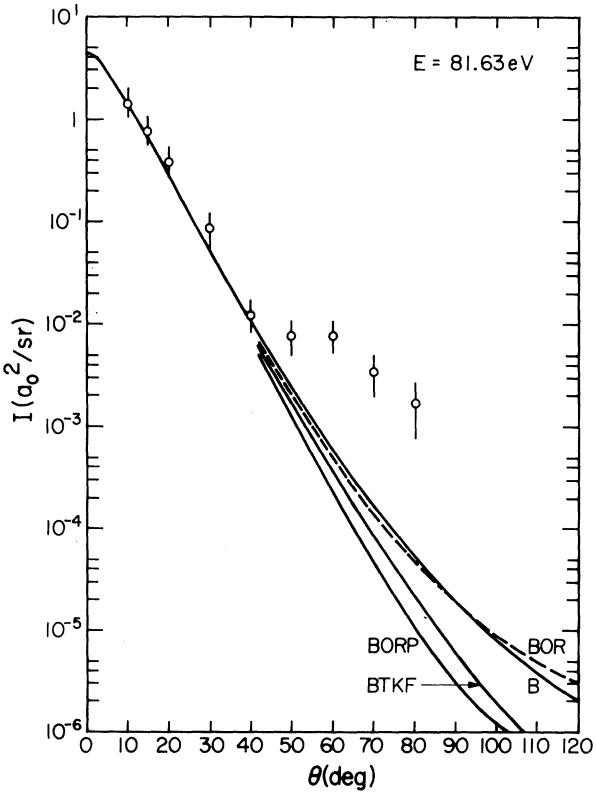

FIG. 6. Theoretical (curves) and experimental (circles with error bars) differential cross sections for excitation of the helium 2^1P state at $E=81.63$ eV. The theoretical curves are calculated from the KI set of ϕ_{0n}. The experimental results have been multiplied by 1.21 for this plot to normalize them to the post BOR approximation at 10°. The prior and post BOR and Born-transferred KF approximate results are not shown at small angles where they are similar to the Born approximation.

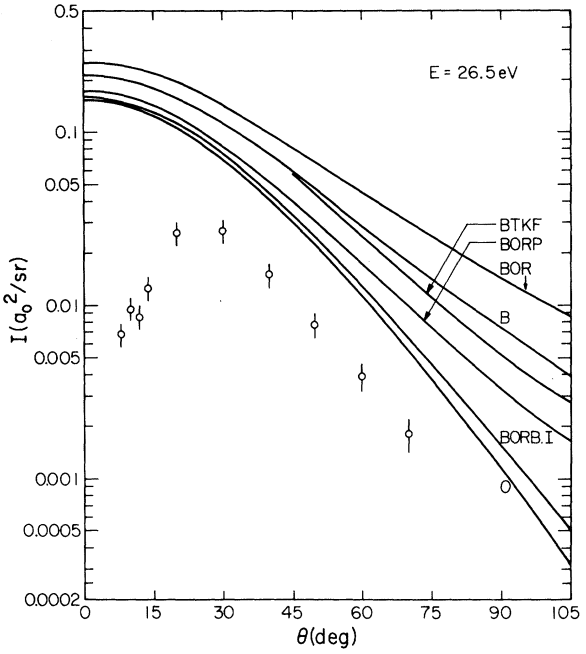

FIG. 7. Experimental differential cross section for excitation of helium to the 2^1P state at 26.5 eV. The cross sections are normalized to the experiment of Jobe and St. John as described in the text (Sec. II B). Several theoretical cross sections are shown for comparison. The BTKF is not shown at small angles where it crosses the B (at 41°) and the BOR (at 8°). The BTVPS approximation is not shown because it differs from the O by only 1–4 % over the range shown. The labels on the curves are summarized in footnote b of Table X.

which can easily be derived from (1) and (11). The three terms of Eq. (12) which contribute to the differential and integral cross sections, are the direct, exchange, and interference terms, respectively. Their sum is denoted as the unpolarized beam cross section or total cross section, which is the one experimentally observed.

We now proceed to define the several G. In the Ochkur approximation[39, 28, 42] it is given by

$$G^{O} = -1/k_0^2 . \tag{14}$$

Rudge modified the Ochkur result so that it can be obtained from a variationally correct expression for the scattering amplitude. The result is [43–46]

$$G = -1/[k_n - i(2U_0)^{1/2}]^2 = -e^{2i\xi_{0n}}(k_n^2 + 2U_0)^{-1}, \tag{15}$$

where $$\xi_{0n} = \arctan[(2U_0)^{1/2}/k_n]. \tag{16}$$

Rudge's result for the exchange amplitude has been called the Ochkur-Rudge approximation. The approximation in which the direct amplitude is calculated in the Born approximation and the exchange amplitude is calculated in the (OR) approximation will be called the Born-Ochkur-Rudge (BOR) approximation. However, Rudge has not used exactly this approximation; rather, he used the OR approximation for the exchange amplitude and a similar result for the direct amplitude.[43, 46] The expressions (9) and (15) are derivable in a prior interaction formulation.[43, 46] We can also obtain from the post interaction formulas[44]

$$G = -1/k_n^2 \tag{17}$$

in the post Ochkur approximation, and

$$G = -1/[k_0 - i(2U_n)^{1/2}]^2 \tag{18}$$

in the post Born-Ochkur-Rudge approximation. There is another modification, due to Bely, which is to take[45]

$$G = -1/(k_n^2 + 2U_0); \tag{19}$$

i.e., G is the negative of the modulus of the complex value it has in the OR approximation. This approximation, in which we use (5) for the direct amplitude and (19) for exchange, we call the symmetrized BOR approximation (or, when referring just to the exchange part, the symmetrized OR approximation).[47] It has the advantage that there is no post-prior discrepancy. (For consistency with the derivation of the Rudge approximation, we use the ionization energy for the calculated wave function employed (see Table III). When k_n is computed from k_0 and the experimental ΔE, this does lead to a very small post-prior discrepancy when approximate wave functions are used. (We use the prior form.) The BOR approximation does not satisfy detailed balancing; the symmetrized BOR cross section does.[45, 26]

Using approximations to the amplitudes in the Coulomb wave approximation, Kang and Foland derived another Ochkurlike relation, i.e., they found that the ratio of their exchange amplitude to their direct amplitude was a quotient which did not depend on the bound-state wave functions.[48] Their relation has no post-prior difference.[48] We use this relation and the Born direct amplitude to obtain an exchange amplitude. We use this exchange amplitude with the Born direct amplitude to calculate the cross sections. We call this the transferred Kang-Foland (TKF) approximation for the exchange part of the scattering and the Born-TKF approximation for the total scattering. The result is again given by Eqs. (11) and (12), but with

TABLE III. Properties for wave functions used in scattering calculations. Energies are given in hartrees and the diamagnetic susceptibility is given in 10^{-6} cm^3/mole.

	1^1S	2^1P	
E (SCF used here [a])	−2.8617	−2.1225	$\Delta E = 0.7392$
U	0.8617	0.1225	
χ_d [b]	−1.8779	−25.5844	
E (Weiss [c])	−2.9037	−2.1238	$\Delta E = 0.7799$
U	0.9037	0.1238	
E (KKB [d, e])	−2.9033	−2.1222	$\Delta E = 0.7811$
U	0.9033	0.1222	
χ_d	−1.890 [f]	−24.3536 [g]	
E (expt [h])	−2.9036	−2.1238	$\Delta E = 0.7797$
χ_d	−1.890 [i]	−24.972 [j]	
E (KK-I [k, e])	−2.9033	−2.1222	$\Delta E = 0.7811$
χ_d	−1.890 [f]	−24.6633	
E (KK-II [k])	−2.8750	−2.1224	$\Delta E = 0.7526$
χ_d	−1.9861	−26.1066 [l]	
E (KK-III [k])	-2.847_5	−2.1222	$\Delta E = 0.7253$
χ_d	−1.6687	−24.3536 [l]	

[a] Reference 59.

[b] This is calculated from $\chi_d = -0.791987 \times 10^{-6} \langle r_1^2 + r_2^2 \rangle$, where r is in a_0 [cf. T. H. Dunning, Jr., N. W. Winter, and B. V. McKoy, J. Chem. Phys. 49, 4128 (1968)].

[c] Reference 58.

[d] Wave functions used by Bell, Kennedy, and Kingston (Ref. 18).

[e] The KKB calculations used in this paper are from Ref. 18 and calculation I of Ref. 17.

[f] Y.-K. Kim and M. Inokuti, Phys. Rev. 165, 39 (1968).

[g] This wave function is written with a sign error in Ref. 18, but is the same wave function as used in calculation III of Ref. 17.

[h] W. C. Martin, J. Res. Natl. Bur. Stds. 64, 19 (1960).

[i] C. L. Pekeris, Phys. Rev. 115, 1216 (1959).

[j] B. Schiff, H. Lifson, C. L. Pekeris, and P. Rabinowitz, Phys. Rev. 140, A1104 (1965).

[k] Wave functions used by Kennedy and Kingston in calculations I, II, and III of Ref. 17.

[l] This wave function is not properly normalized in Table I of Ref. 17.

$$G = G^{O} C_{KF}, \tag{20}$$

where G^{O} is defined in Eq. (9) and[48]

$$C_{KF} = \left(\frac{\gamma}{\alpha}\right)^{i/k_0} \left(\frac{\alpha+\beta}{\alpha}\right)^{i/k_n} \left[F\left(1 - i/k_0, 1, \frac{2i(k_0 k_n - \vec{k}_0 \cdot \vec{k}_n)}{k_0^2 k_n}\right) \Big/ F(i/k_0, i/k_n, 1; \chi)\right] \tag{21}$$

and

$$\alpha = \tfrac{1}{2} q^2 , \tag{22}$$

$$\beta = k_0 k_n \cos\theta - k_n^2 , \tag{23}$$

$$\gamma = \tfrac{1}{2}(k_0^2 - k_n^2) , \tag{24}$$

$$\chi = 2k_0 k_n (\cos\theta - 1)/(k_0 - k_n)^2 . \tag{25}$$

$F(u, v, x)$ and $F(u, v, w; x)$ in Eq. (21) denote the confluent hypergeometric function and the hypergeometric function, respectively.[49] Equations (20) and (21) are equivalent to writing

$$g = f^{B}(q^2/k_0^2) C_{KF}, \tag{26}$$

where f^{B} is defined in Eq. (4). In the high-energy limit, the complex number C_{KF} approaches 1, and Eqs. (20) – (26) become the Ochkur-Bonham approximation. Kang and Foland do not use any explicitly energy-dependent approximations, however,

and Eq. (26) is claimed to be valid at all energies.[48]

Presnyakov, Sobelman, Vainshtein, and Opykhtin[50–52] attempted to derive an expression for the cross section that takes account of electron-electron repulsion as much as possible. They made several mathematical approximations[53] which have been variously criticized.[54, 55] However, the method has been shown to give good integral cross sections even at intermediate energies.[51, 52, 56] In addition, by taking the ratio of their exchange scattering amplitude g^{VPS} to their direct scattering amplitude f^{VPS}, we find it yields a relatively simple Ochkur-like relation. We can use this ratio and the Born direct amplitude to obtain yet another approximation to the exchange amplitude. We call this amplitude the transferred Vainshtein-Presnyakov-Sobelman (VPS) method; that is

$$g = (g^{\mathrm{VPS}}/f^{\mathrm{VPS}})f^{\mathrm{B}} \tag{27}$$

or

$$G = C_{\mathrm{TVPS}} G^{\mathrm{O}}, \tag{28}$$

where
$$C_{\mathrm{TVPS}} = \frac{F(-i\nu, i\nu, 1, \frac{1}{4})}{F(-i\nu, i\nu, 1, \chi)}, \tag{29}$$

and
$$\chi \equiv \frac{2\Delta E + q^2}{2\Delta E + 3q^2}, \tag{30}$$

$$\nu = [k_0 + \sqrt{(2U_0)}]^{-1}. \tag{31}$$

We use the transferred VPS exchange amplitude with the Born direct amplitude as the Born-transferred VPS approximation. Equation (31) includes their correction for a real (not complex) "effective charge."[50–52] Crothers made a suggestion[57] which is equivalent to replacing G^{O} by the prior OR approximation for G in Eq. (28), but we do not use that approximation. We do not attempt to justify the severe mathematical approximations in the VPS formalism except to test empirically how good are the results of the transferred VPS approximation (where some of the errors cancel) for integral and differential cross sections.

C. Generalized Oscillator Strengths

The expression (11) for the cross section requires the generalized oscillator strength $\phi_{0n}(q)$. We used two sets of $\phi_{0n}(q)$ for our calculations. The first set was computed by Kim and Inokuti[19] using Weiss's 52- and 53-term Hylleraas type wave functions.[58] These ϕ_{0n} are probably accurate within a few percent.[19] The second set was computed by us using SCF wave functions in the optimized-exponent-double-ζ approximation for both the ground and excited states. These wave functions[59] are of the form

$$\Psi_0 = \varphi_0(r_1)\varphi_0(r_2), \tag{32}$$

$$\Psi_n = (\sqrt{2})^{-1}[\varphi_1(r_1)\varphi_2(\vec{r}_2) + \varphi_1(r_2)\varphi_2(\vec{r}_1)], \tag{33}$$

where
$$\varphi_i(r_2) = \sum_{j=1}^{2} c_{ji}\chi_{1ji}(r_2), \quad i = 0, 1 \tag{34a}$$

$$\varphi_2(\vec{r}_2) = \sum_{j=1}^{2} c_{j2}\chi_{2j2}(r_2)\cos\theta_2, \tag{34b}$$

and
$$\chi_{njl}(r) = \sqrt{(k_{ji}^3/\pi)}\,(rk_{ji})^{n-1}e^{-k_{ji}r}, \tag{35}$$

with n being the principal quantum number. The best coefficients and exponents are given in Table IV and the energies in Table III. Using Eqs. (10), (6), and(7), we find

$$\phi_{0n}(q) = \frac{4}{q^2}\,\Delta E\Big[\int \varphi_1(r_2)\varphi_0(r_2)dr_2 \times \int \varphi_2(\vec{r}_1)e^{i\vec{q}\cdot\vec{r}_1}\varphi_0(r_1)d\vec{r}_1\Big]^2. \tag{36}$$

The first integral equals 0.983277, and the second integral is evaluated analytically at each desired q. In this expression we used the theoretical $\Delta E = 0.739220$.

The calculations of generalized oscillator strengths are known to be sensitive to the accuracy of the description of the bound charge distributions by the approximate wave functions.[60, 61] To illustrate the accuracy of the wave functions used here, we have calculated the diamagnetic susceptibilities from some of them and list these values in Table III. This property is proportional to $\langle r_2^2\rangle$, and Table III shows that the present SCF wave functions give fairly accurate values. The use of a GF, instead of a Hartree-Fock, ground-state wave function would have changed the SCF values to $\chi = -1.915\times10^{-6}$ cc/mole and $\Delta E = 0.7555$ hartree.[62] It is expected that correlated wave functions should not be necessary for the description of elastic scattering because the Born elastic cross sec-

TABLE IV. Parameters and coefficients for SCF wave functions for 1^1S and 2^1P states.

i	0	1	2
c_{1i}	0.835 188	1.010 481	1.019 323
c_{2i}	0.189 650	−0.010 996	−0.027 347
k_{1i}	1.446	2.012	0.493
k_{2i}	2.870	2.874	1.037

tions depend on a property (the Fourier transform) of the electron density, and SCF wave functions predict the diagonal matrix element of such one-electron operators correct through first order (Brillouin's Theorem).[63] Another approximate wave function, which accounts for only part of the electron correlation, does not necessarily improve the description of the electron-density property. These expectations have been confirmed numerically by Hurst, and Kolos and Pecul.[60] Inelastic scattering depends, however, on the transition electron density [cf. Eq. (7)]. This is an off-diagonal element of a one-electron operator, and its accuracy is not insured by Brillouin's Theorem. Nevertheless, we expect that the accuracy of the description of the stationary charge densities will generally be an important indication of what accuracy to expect in the scattering calculation, and that is why we consider $\langle r_2^2 \rangle$ to be relevant.[61]

Since the calculations require many values of $\phi_{0n}(q)$ at irregular values of q, we found it most convenient to fit $\phi_{0n}(q)$ to an analytic expression as a function of q. Lassettre[64] noted that a Maclaurin power series in q is not convergent in the whole range of physically attainable q. He introduced[64] a power-series representation of $\phi_{0n}(q)$ in the variable $x/(1+x)$, where

$$x = q^2/\alpha^2 \tag{37}$$

and

$$\alpha = (2U_0)^{1/2} + (2U_n)^{1/2} \ . \tag{38}$$

This series is convergent in the entire physical domain. The details of the application of this expansion to $S \rightarrow P$ transitions in atoms were worked out by Vriens.[65] In this case,[65]

$$\phi_{0n}(q) = \frac{\phi_{0n}(0)}{(1+\nu)^6}\left[1 + \sum_{\nu=1}^{N} C_\nu \left(\frac{x}{1+x}\right)^2\right] , \tag{39}$$

where $N = \infty$ for the exact result. We found that Eq. (39), with $N = 4$–6, was a very convenient and accurate expression for fitting $\phi_{0n}(q)$ over a finite range of q. It is perhaps not surprising that the series is rapidly convergent, since Lassettre[64] noted its relation to the Euler transformation, which is sometimes used to speed convergence. The fitting procedure with this expression was very well behaved. Also, the fits were found to have the property that a fit to data in the range $q = 0$ to q_f gave good $\phi_{0n}(q)$ even for $q > q_f$; i.e. the fits could be used to extrapolate. However, this does lower the accuracy. The parameters for three such fits, which we used to compute the differential cross section, are given in the Appendix. For the $\phi_{0n}(q)$ calculated from Eq. (36), we also computed the differential cross section using a completely independent program which used $\phi_{0n}(q)$ directly. The agreement between the two procedures was excellent. Note that the C_ν obtained in our least-squares fits over a finite range of q with finite N may not be good approximations to the theoretically calculable values in the exact expression with $N = \infty$.

We would like to point out the advantages of this procedure for calculations on larger atoms and on molecules. In that case, a considerable effort may be required to calculate ϕ_{0n} at one q. Then one should calculate a set of $\phi_{0n}(q)$ at *evenly spaced* values of q over the range from $q^2 = 0$ to the highest q^2 of interest and fit this set to a series such as (38). Then the series can be used to obtain ϕ_{0n} at all the other q's needed to calculate differential cross sections.

D. Comparison of Results Obtained with Different Wave Functions

At an impact energy E and scattering angle θ, the momentum transfer is given by

$$q = (2k_0^2 - \Delta E - 2k_0 k_n \cos\theta)^{1/2} \ , \tag{40}$$

$$\text{with} \quad k_n = (k_0^2 - \Delta E)^{1/2} \ . \tag{41}$$

For the calculations with very accurate wave functions, the use of either the experimental or theoretical ΔE will give the same results. In order to obtain correct thresholds, etc., when using inaccurate wave functions, the experimental ΔE is usually used to compute q^2. For our calculations with the SCF wave functions, we computed the cross sections using both the experimental and theoretical ΔE (see Table III). Some results in the Born approximation computed each way are shown in Table V. The differences are quite large, especially at small angles. It is probably more consistent to use the experimental ΔE because this corresponds to using trial functions (plane waves) with the same asymptotic behavior as the exact wave functions for the actual physical process. The small q generalized oscillator strength is expected to be too large when ΔE (theoretical) is used, because the 2^1P wave function is too expanded (cf. Table III). Table III shows, however, that using ΔE (expt) is in the right direction to correct this. Similarly, this argument predicts that the Kennedy-Kingston calculation I[17] would be corrected for small q since the 2^1P wave function is too contracted but ΔE (theoretical) is too large (cf. Table III). We will use only the experimental ΔE in the rest of this paper.

Also shown in Table V are some Born cross sec-

TABLE V. Born differential and integral cross sections (a_0^2). (Number in parentheses is power of ten by which value given is to be multiplied.)

ϕ_{0n} ΔE		SCF [a] theor	SCF [a] expt	KKB [a] expt	KI [a] expt
E (eV)	θ (deg)				
25	0	2.17(−1)	1.30(−1)	1.56(−1)	1.44(−1)
	60	3.26(−2)	2.64(−2)	3.16(−2)	2.86(−2)
	120	3.02(−3)	3.13(−3)	3.69(−3)	3.24(−3)
	180	1.23(−3)	1.37(−3)	1.60(−3)	1.40(−3)
	integral	3.60(−1)	2.64(−1)	3.17(−1)	2.88(−1)
50	0	2.00	1.58	1.89	1.79
	60	5.14(−3)	4.95(−3)	5.82(−3)	5.11(−3)
	120	5.45(−5)	5.47(−5)	5.90(−5)	4.82(−5)
	180	1.30(−5)	1.32(−5)	1.34(−5)	1.07(−5)
	integral	5.55(−1)	4.78(−1)	5.73(−1)	5.32(−1)
136	0	9.32	7.79	9.28	8.84
	60	4.73(−5)	4.55(−5)	4.84(−5)	3.93(−5)
	120	1.12(−7)	1.09(−7)	8.92(−8)	6.80(−8)
	180	1.94(−8)	1.88(−8)	1.46(−8)	1.10(−8)
	integral	4.06(−1)	3.65(−1)	4.36(−1)	4.10(−1)

[a]See Appendix.

tions computed from the Kennedy-Kingston-Bell (KKB) and Kim-Inokuti (KI) generalized oscillator strengths (see Appendix). The differences are larger than expected, but the Kennedy and Kingston results[17] are about 4% higher than the more accurate (KI) calculations[19] and the Bell *et al*. results[18] are even higher. Also, Kennedy, Kingston, and Bell do not give $\phi_{0n}(q)$ for high enough q for us to get a good fit over the whole range needed for these calculations. This explains the differences and we will not consider our calculations with the KKB set of $\phi_{0n}(q)$ in any more detail. Our fit to the generalized oscillator strengths of Kim and Inokuti is quite accurate, and they claim an accuracy of 1% for their generalized oscillator strengths. An interesting comparison is that our computed Born integral cross sections computed from the KI generalized oscillator strengths agree with those computed and published by Kennedy and Kingston[17] to within $3\frac{1}{2}$% up to the highest energy they considered, 245 eV. Above this energy our integral cross sections computed from the KI generalized oscillator strengths agree with the less accurate ones published by Bell *et al.*[18] within 8% up to 1000 eV.

A comparison of the generalized oscillator strengths from the SCF calculation with those of Kim and Inokuti[19] shows that the SCF ϕ_{0n} is 12% too low at $q^2=0$ (see Appendix) but falls less rapidly with increasing momentum transfer. Thus, for example, the SCF ϕ_{0n} are 9% lower at $q^2=1.0$, about correct at $q^2=4.6$, 10% too high at $q^2=7.3$, and 53% too high at $q^2=40$. Thus, the answer to the question about the comparison suggested by Kim and Inokuti[19] is that our SCF results are apparently not quite as accurate as the results of Altshuler[66] for small q. This must be due to some fortunate cancellation of errors in Altshuler's calculations, since his wave functions are less accurate. [Altshuler used the same wave functions as used by Kingston and Kennedy[17] in their calculation III (see Table III)]. The differences between the SCF and accurate results means the SCF will predict a differential cross section falling too slowly with angle compared to the exact Born result (see, e.g., Table VI, and an integral cross section, which is everywhere too small, compared to the exact Born result (this is because the integral cross section is sensitive to small angles where the differential cross section is large). The integral cross sections are compared more quantitatively in Sec. IV.

The direction of deviation of the SCF result is expected (cf. Hurst[60]). SCF wave functions are usually too large for large r and too small for small r. Thus, because the r derivative of the wave function is larger for small r, the generalized oscillator-strength Fourier transform is generally too large for small q and too small for large q.

IV. INTEGRAL CROSS SECTIONS

Figures 8–10 compare the integral cross sections $Q(E)$ computed in the various approximations with the experimental results of Jobe and St. John.[2] At intermediate energies all our theoretical integral cross sections are too large. For all our sets of ϕ_{0n}, we find that the following sequence of the theories puts the cross-sections in decreasing

TABLE VI. Comparison of differential cross section (in a_0^2) for excitation of 2^1P state as computed with different wave functions. $E=60$ eV. (The number in parentheses indicates the power of 10 by which the number is to be multiplied.

Method	Born		prior Born-Ochkur-Rudge	
θ	SCF [a]	KI [a]	SCF [a]	KI [a]
0°	2.27	2.56	2.25	2.54
10°	1.18	1.33	1.16	1.31
20°	3.47(−1)	3.87(−1)	3.38(−1)	3.77(−1)
30°	9.48(−2)	1.04(−1)	9.10(−2)	9.96(−2)
60°	2.36(−3)	2.40(−3)	2.32(−3)	2.35(−3)
80°	3.06(−4)	2.92(−4)	3.46(−4)	3.30(−4)
100°	6.09(−5)	5.38(−5)	8.67(−5)	7.65(−5)
140°	7.82(−6)	6.14(−6)	1.76(−5)	1.38(−5)
180°	4.04(−6)	3.05(−6)	1.08(−5)	8.20(−6)

[a]See Appendix.

order at all energies: prior Born-Ochkur-Rudge (BOR) approximation, Born-transferred Kang-Foland (BTKF) approximation, post Born-Ochkur-Rudge (BORP) approximation, symmetrized (BORB. I) approximation, Born-transferred Vainshtein-Bresnyakov-Sobelman (BTVPS) approximation, and prior Ochkur (O) approximation. There is a larger gap between the BORP approximation and the BTKF approximation than between the others. In addition, the Born (B) approximation integral cross section fits into this scheme around the BTKF approximation and BOR approximation results. (The last four cross sections in the list will be called the group i_1. The post Ochkur (OP) approximation is also included in group i_1, and group i_2 comprises the Born, BOR and BTKF approximations.)

That these Born-like approximations predict cross sections that are too large might have been expected due to the lack of back coupling of the final state to the initial state. It was also previously recognized that the Born approximation for n^1P excitation in helium predicted an integral cross-section curve which disagreed with experiment in that it looked too much like the experimental curves for n^3P excitation (i.e., it was peaked too close to threshold).[2,67] However, these conclusions were tempered by doubts about the validity of the approximate helium wave functions.[67] Figures 8–10 show that this error is still there when the accurate KI generalized oscillator strengths are used and also when Ochkurlike corrections are made to include exchange effects. However, the group i_1 approximations give considerable improvement over the Born approximation in the shape of the cross section curve. The agreement in magnitude is also better; in the most favorable case, the peak of the post Ochkur approximation integral cross section, as computed from the SCF generalized oscillator strengths, is only 28% higher than the experimental maximum Q.

Moiseiwitsch and Smith[68] noted that for excitation

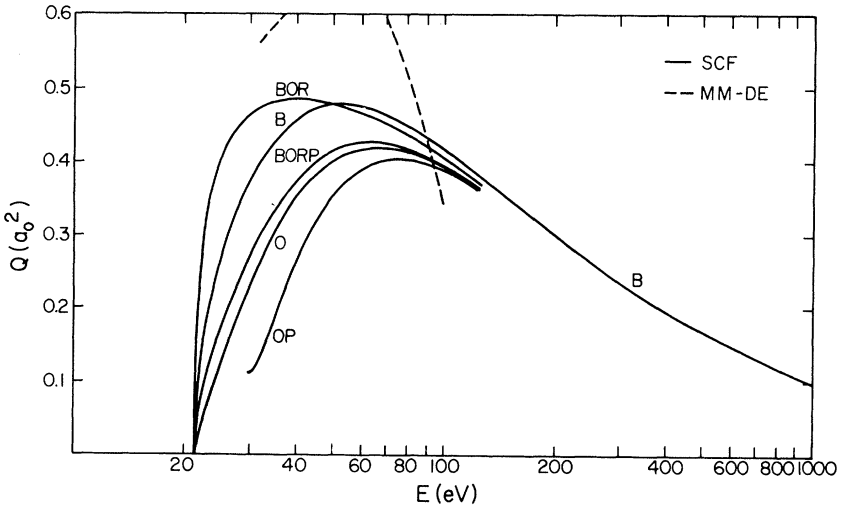

FIG. 8. Integral cross sections for excitation of the helium 2^1P state computed from SCF wave-functions set of generalized oscillator strengths. The OP curve is not shown below 30 eV, where it has a peak which would put it off scale on this plot (see text). The BTVPS approximation is not shown because it is within about $\frac{1}{2}$% of the O curve. Above 125 eV, where all these approximations give similar results, only the Born approximation is shown. The figure also shows the distorted wave plus exchange results (DE) of Massey and Mohr (using simple wave functions) as a dashed line (from Ref. 77).

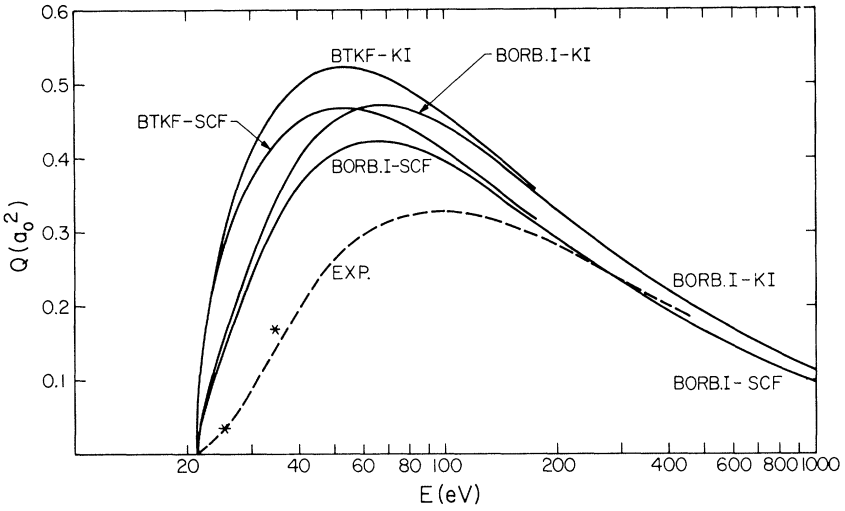

FIG. 9. Comparison of integral total cross sections for excitation of the helium 2^1P state computed from the SCF and KI sets of ϕ_{0n}. The experimental cross section (Ref. 2) is also shown up to 450 eV. The BTKF results are not shown above 175 eV where they are within 1.3 % of the symmetrized Born-Ochkur-Rudge (BORB.I) cross sections. The asterisks show the theoretical results of Vainshtein and Dolgov (Ref. 75) at the two highest energies they considered.

of the 3^1P state of He the cross sections determined by the method used by Miller, St. John, Lin, and Jobe are "characterized by smaller initial slopes and...lower peaks shifted to higher energies than...the results of other workers." If this represents a systematic error, then the agreement of our theoretical results with experiment is better than it appears here.

The post Ochkur approximation predicts a large peak at threshold. This is shown by Eq. (17) and Table VII. Although experiments with good incident-energy resolution have shown[69, 70] that the excitation function for helium 2^1P lines does have a small narrow maximum near 22.5–23.8 eV, the peak predicted by the post Ochkur approximation is much too large and appears to be spurious. It is analogous to the too large elastic cross sections predicted by the prior Ochkur method near zero energy.[26] As in that case, the difficulty is alleviated by the Rudge modification of the exchange amplitude (cf. integral cross sections computed from the post Ochkur and post BOR approximations in Table VII).

Figures 8–10 confirm the conclusion of Bell *et al.*[28] that the prior Ochkur approximation is better than the (prior) BOR or Born approximation for $Q(E)$ in this case. Of all the cross sections examined here, the prior Ochkur and BTVPS approximations give best agreement with $Q(E)$ over the whole energy range.

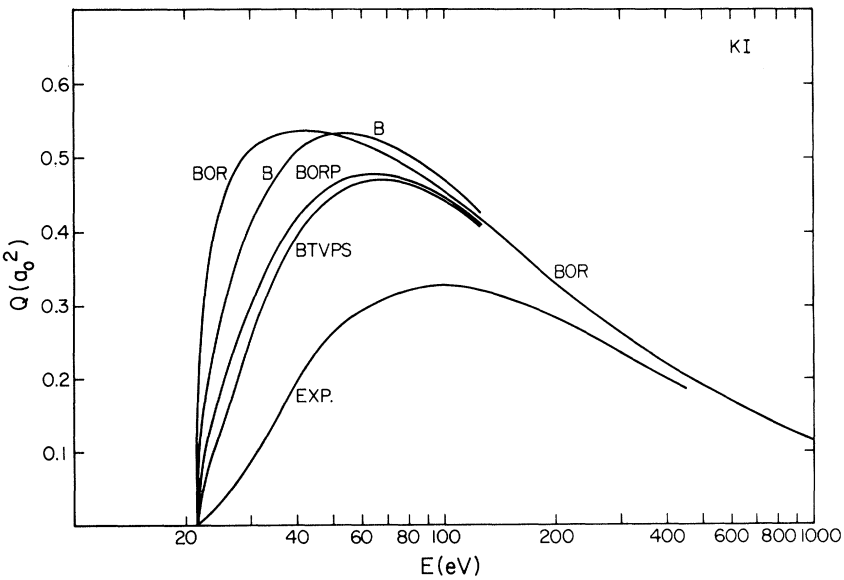

FIG. 10. Integral total cross sections for excitation of the helium 2^1P state computed from the KI set of ϕ_{0n}. The experimental cross section (Ref. 2) up to 450 eV is also shown. The prior Ochkur approximation cross section (not shown) is within $\frac{1}{2}$% of the BTVPS. The post Ochkur approximation cross section (not shown) is below the BTVPS at energies more than 6 eV above threshold.

TABLE VII. Some total excitation cross sections (in a_0^2) computed from Kim-Inokuti generalized oscillator strengths. (The number in parentheses indicates the power of 10 by which the number is to be multiplied.)

E (eV)	Born approximation (B)	Ochkur approximation (prior) (O)	Ochkur approximation (post) (OP)	Born-Ochkur-Rudge approximation (post) (BORP)	Born-transferred KF approximation (BTKF)
21.6	9.29(−2)	2.59(−2)	6.37(1)	5.29(−2)	1.07(−1)
22.0	1.33(−1)	4.09(−2)	1.94(1)	7.73(−2)	1.51(−1)
25.0	2.88(−1)	1.35(−1)	6.92(−1)	1.89(−1)	2.95(−1)
27.0	3.48(−1)	1.89(−1)	2.03(−1)	2.41(−1)	3.50(−1)
30.0	4.11(−1)	2.59(−1)	1.19(−1)	3.02(−1)	4.07(−1)
35.0	4.74(−1)	3.39(−1)	2.07(−1)	3.74(−1)	4.66(−1)
80.0	5.02(−1)	4.63(−1)	4.50(−1)	4.68(−1)	4.92(−1)

V. DIFFERENTIAL CROSS SECTIONS

A. Comparison of Calculations with Experiment

Vriens *et al.*[7] reported some small-angle differential cross sections at 100–400 eV (see Table I). At energies 175 eV and lower, they found deviations in shape from their semiempirically determined Born cross sections. We compared their data to the cross sections we computed from the KI generalized oscillator strengths and find the same conclusions still hold. The Born-approximation differential cross section falls less rapidly with angle than the experimental one. However, inclusion of exchange via one of the Ochkurlike relations (their predictions are all similar in this case) makes little difference at the higher of these energies (above 200 eV), but at least halves the discrepancy in the shape of the lower energy differential cross sections. For example, the shape of the (prior) BOR differential cross section is within their experimental error at every point. Above 49 eV the BOR differential cross section falls more rapidly with angle than does the Born approximation differential cross section. Below 49 eV this situation is reversed.

Figures 3–6 compare the theoretical differential cross sections using the Kim-Inokuti set of generalized oscillator strengths with our experimental ones in the energy range 34–81.63 eV. At each energy are shown the experimental differential cross section and the four or more (out of eight considered) theoretical cross sections which agree best in shape (except as indicated otherwise in the captions). In each figure the experimental cross section (normalized as explained in Sec. II B) is renormalized at 10° to the BORP cross section. At the lower of these energies the theoretical differential cross section has the right shape out to about 40°, and after that it falls too rapidly. At the higher energies the theoretical differential cross section begins to fail at even smaller angles. This is discussed in more detail in Sec. V B. As discussed in Sec. III D, the differential cross sections computed from the SCF set of generalized oscillator strengths do not fall as rapidly with angle. Thus, these approximate results are in better agreement with experiment than are the results computed from the KI generalized oscillator strengths. This is illustrated by Table VIII.

The conclusion that the Born approximation predicts a cross section which falls too rapidly with angle in this energy range could also have been drawn from the work of Jusick, Watson, Peterson, and Green.[71] However, their analysis is based on old (1932–1933) data which is inaccurate (see Sec. I and Ref. 1) and the validity of their results is thereby questionable.

Of all the theoretical methods we are considering, the (prior) BOR approximation gives the differential cross section which is in best agreement with the shape of the experimental one in this energy range (34–82 eV). Further, only this method of including exchange improves the Born approximation (no exchange) for the shape of this intermediate energy differential cross section.

At high enough energies (above about 26 eV), the prior Ochkur total amplitude, proportional to

$$2/q^2 - 1/k_0^2 ,$$

has a zero. As the energy is increased, this zero, which causes a sharp dip to zero in the predicted differential cross section, moves in from 180° until, in the high energy limit, it is at 90° This dip is shown in Figs. 11 and 12. This dip in the differential cross section is a peculiarity of the prior Ochkur approximation not only for this transition but for all electron scattering processes which involve both direct and exchange scattering. A very similar dip occurs in the BTVPS and symmetrized Born-Ochkur-Rudge (BORB. I) approximations.[72] In the post Ochkur approximation there is an analogous dip which comes in from small angles and moves out to 90° in the high-energy limit. This dip can be seen in Figs. 5, 11, and 12 and is re-

TABLE VIII. Ratio $I(E, 10°)/I(E, 60°)$ of differential cross sections for excitation of the 2^1P state of He as computed from two different sets of generalized oscillator strengths[a] and from experiment.

E	B	O	Born-Ochkur-Rudge approximation (prior) (BOR)	OP	BORP	Symmetrized Born-Ochkur-Rudge approximation (BORB. I)	BTKF	Born-transferred VPS approximation (BTVPS)	Expt.
KI									
26.5	6.8	12	5.3	0.3	9.2	11	9.5	13	4.1
34	29	63	23	82903	46	57	42	63	54
44	114	284	98	1765	210	261	174	288	45
55.5	375	1023	362	3122	770	948	589	1035	41
81.63	2505	7627	2992	14310	6017	7190	4042	7724	
SCF									
26.5	6.6	12	5.2	0.3	8.9	11	9.2	12	4.1
34	27	60	21	78579	43	54	40	60	54
44	106	264	91	1638	194	242	162	267	45
55.5	340	929	329	2838	700	861	535	941	41
81.63	2169	6600	2590	12379	5207	6219	3499	6687	

[a]The ratios computed from the Bell, Kennedy, and Kingston set are very similar to those from the SCF set but a little higher.

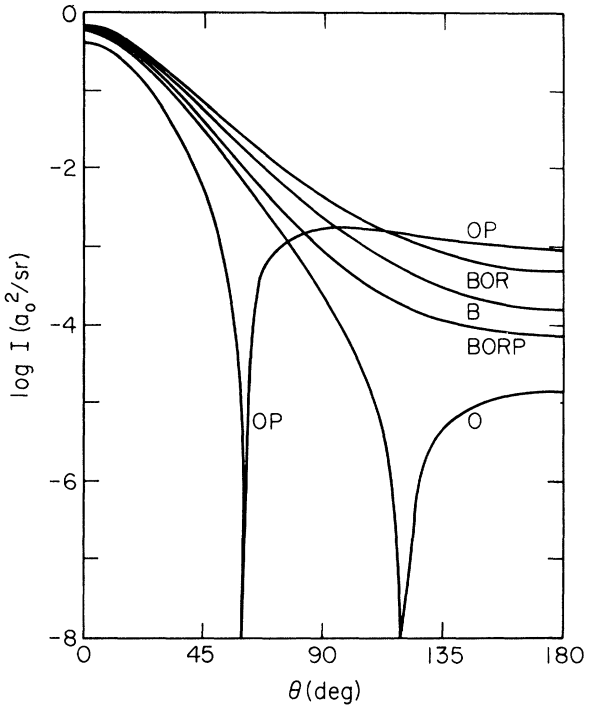

FIG. 11. Theoretical differential total cross sections for excitation of the 2^1P state of helium at $E = 34$ eV. These are computed from the KI set of generalized oscillator strengths. The curve labels for Figs. 11–15 are defined in the first paragraph of Sec. IV. (The logarithm is to the base 10.)

sponsible for the fact that the post Ochkur approximation disagrees so violently with our experiments (cf. Table VIII). There are no dips like this in the Born, prior or post BOR, or BTKF approximations. This is illustrated by Figs. 11–15. The comparison with our experiments at 10°–80° suggests that the dip is an artifact of these approximations, and that the prior and post Ochkur, symmetrized OR, and transferred VPS Ochkur-like relations cannot be used with the Born amplitude to predict angular distributions which are accurate over the whole angular range.

The experimental 2^1P cross section has a peak at 23° at $E = 26.5$ eV, as shown in Fig. 7. Seven of the theoretical cross sections we computed are monotonically decreasing from 0°–150° at this energy (the post Ochkur approximation has a ridiculous shape at this energy for reasons already discussed). Therefore, these first-order calculations do not appear to be as useful so close to threshold.

B. Theoretical Discussion of Calculations

1. *Distortion*

Rothenstein calculated the cross sections for excitation of the 2^1P state of helium by using a clo-

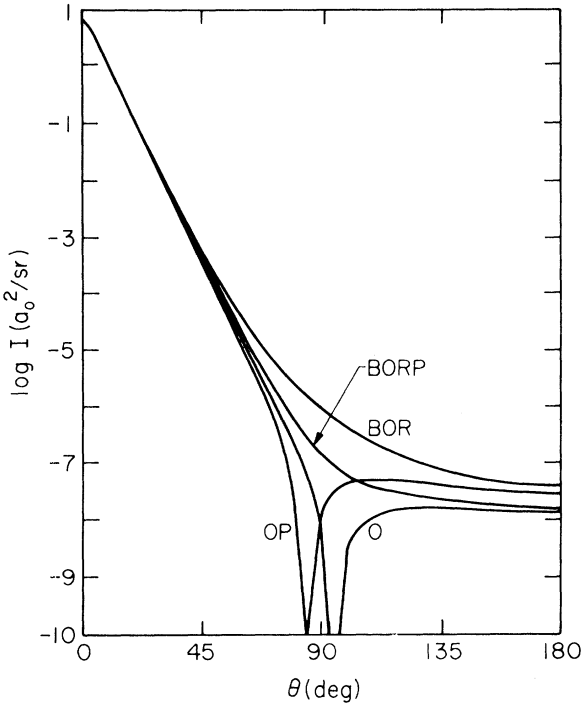

FIG. 12. Theoretical differential cross section for helium 2^1P excitation at $E = 125$ eV (computed from the KI set of generalized oscillator strengths). (The logarithm is to the base 10.)

sure relation to approximate the second Born approximation ($B2$).[73] The $B2$ approximation does not include exchange. His integral cross section shows a smaller peak shifted to higher energies in comparison with the first Born approximation. He also showed that the first Born approximation overestimates the small angle scattering. Thus, both his integral and differential cross sections are in better agreement with experiment than the first Born approximation. Unfortunately, it has been pointed out[74] that the use of the closure relation this way does not lead to a good approximation to the second Born approximation.

Vainshtein and Dolgov[75] calculated the $1^1S - 2^1P$ excitation cross section in the two-state close coupling approximation without exchange. The energy dependence of their cross sections is unusual. Their values for the integral cross sections at 25.11 and 34.81 eV are shown in Fig. 9. The good agreement with experiment is probably fortuitous.

Massey and Mohr calculated the integral cross sections for excitation of the 2^1P state using the prior BO approximation[76] and using a distorted wave method with exchange.[77] They used the simplest Hylleraas wave function for the ground state and the simplest Eckart-type wave function for the 2^1P state. Fundaminsky[78,79] also calculated the excitation cross section in the Born approximation, the BO approximation, and the post Born-Oppenheimer (BOP) approximation. He used similar simple wave functions. Massey and Mohr, and Fundaminsky found that the BO approximation leads to a cross section which rises too rapidly at threshold and is fairly constant in the range 25–45 eV. Fundaminsky found that the BO and BOP approximations are much too large below 30 eV and are about two and three times bigger, respectively, than the Born approximation at energies near threshold. Fundaminsky found the BO agreed well with the Born approximation at 32 eV and the BOP was only 17% larger there. The BO approximation appears to be better for $S \rightarrow P$ transitions than for $S \rightarrow S$ transitions.[80]

The distorted wave plus exchange calculation of Massey and Mohr[77] gives such a large integral cross section that it goes off scale in Fig. 8 in the region 37–69 eV. Massey and Mohr also calculated the differential cross section at 33 and 50 eV in the Born approximation, a distorted wave approximation without exchange, and the distorted wave plus exchange approximation.[77] They presented these in arbitrary units. We have normalized all three of their 33 eV calculations by normalizing their 33-eV Born-approximation cross section to our Born-approximation calculation of

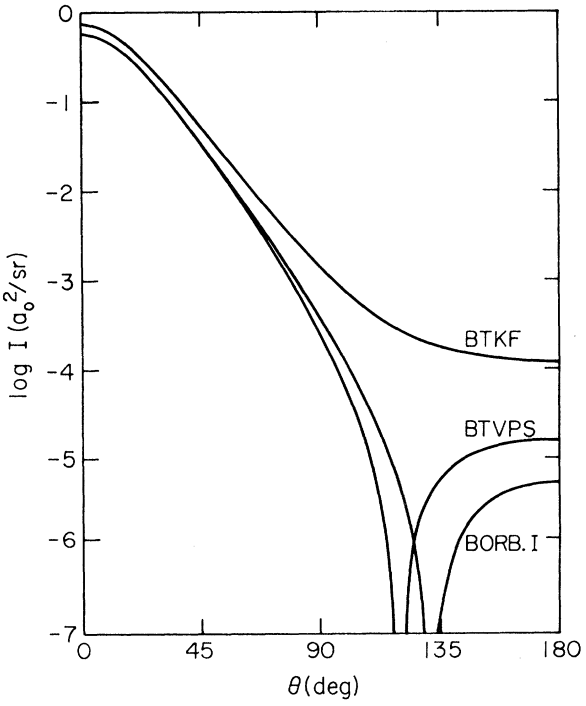

FIG. 13. Theoretical differential cross sections for helium 2^1P excitation at $E = 34$ eV (computed from the KI set of generalized oscillator strengths). (The logarithm is to the base 10.)

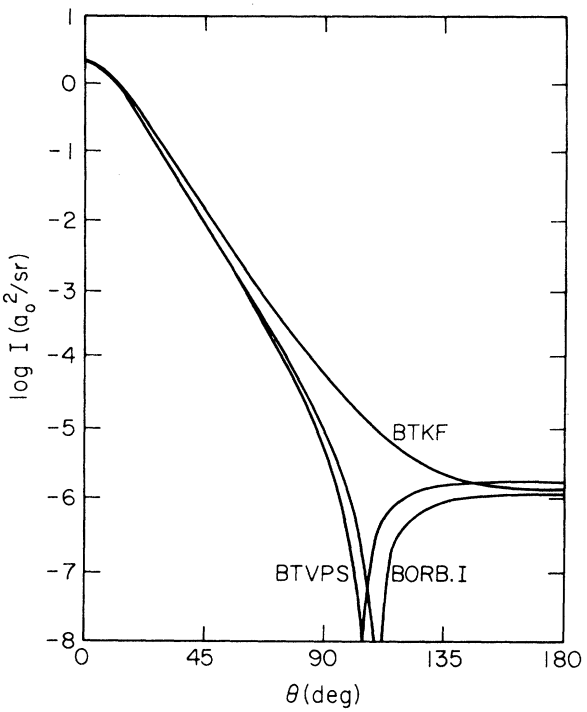

FIG. 14. Theoretical differential cross sections for helium 2^1P excitation at $E = 55.5$ eV (computed from the KI set of generalized oscillator strengths). (The logarithm is to the base 10.)

I (33 eV, 10°) = $0.494a_0^2$/sr from the KI set of generalized oscillator strengths. The three differential cross sections are then presented in Fig. 16 for comparison with our 34-eV experimental results. Their distorted wave plus exchange calculation at 50 eV is compared with our calculations in Table IX. Figure 16 and Table IX both show that inclusion of distortion and exchange change the shape of the predicted large-angle differential cross section in the right direction for better agreement with experiment. The correction for exchange is different in the presence of distortion, and this is an important part of the change.[81] Since Massey and Mohr made many numerical approximations in their calculations, it would be very worthwhile to do accurate distorted wave and distorted wave plus exchange calculations now.

Burke, Cooper, and Ormande[82] made close-coupling calculations on He including the ground state and all single excitations from the ground state to $n = 2$ levels. One of the possibly important assumptions in this calculation is the approximate nature of their bound-state wave functions. Unfortunately they made no calculations at energies more than a volt above threshold for the 2^1P state. While we do not expect our first-order calculations to be valid at such low energies, a comparison of our calculations with those of Burke, Cooper, and Ormande is presented in Table X because this comparison is particularly sensitive to errors in the exchange cross sections and shows that some of our calculations are not even approximately accurate near threshold. For the integral cross section prediction near threshold, the prior Ochkur, BORB. I, and BTVPS approximations are probably the most useful of the theories we used.

2. *Success of First-Order Approximation at Small Momentum Transfer*

The fact that these first-order approximations are approximately valid to higher scattering angles at lower incident energies than higher ones is an indication that the Born approximation is not only a high-energy approximation but also a small momentum-transfer approximation.[83] The angular range over which the Born or (prior) BOR approximation predicts the correct shape of the DCS is approximately the same and can be quantitatively ascertained by normalizing theory to experiment in

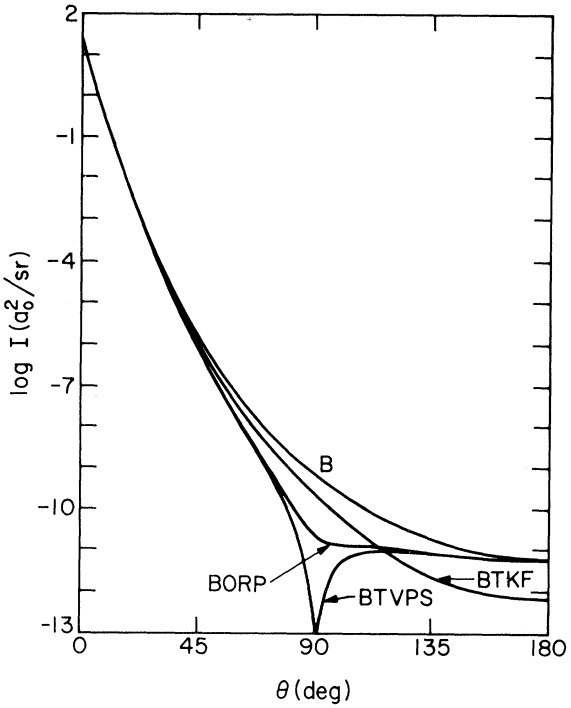

FIG. 15. Theoretical differential cross sections for helium 2^1P excitation at $E = 400$ eV. These are computed from the KI set of generalized oscillator strengths. At this energy, the prior BOR approximation (not shown) is similar to the BTKF for 0–105° and similar to the B for 135–180°. The prior and post Ochkur and symmetrized BOR approximations need not be shown because they are very similar to the BTVPS over the whole angular range at this energy. (The logarithm is to the base 10.)

TABLE IX. Differential cross section ratios at $E = 50$ eV from Massey and Mohr (MM), Ref. 77, and present calculations using SCF, Bell-Kennedy-Kingston (BKK), and Kim-Inokuti (KI) sets of generalized oscillator strengths. (Numbers in parentheses are the power of 10 by which the ratio given is to be multiplied.)

ϕ_{0n} Method[b]	MM a	SCF B	BKK B	KI B	KI BOR	KI BTKF	KI O	KI OP	KI BORB.I	KI BORP
$I(60°)/I(10°)$	6.5(−2)	4.9(−3)	4.9(−3)	4.5(−3)	5.0(−3)	2.9(−3)	1.7(−3)	4.4(−4)	1.9(−3)	2.3(−3)
$I(120°)/I(10°)$	3.9(−2)	5.5(−5)	4.9(−5)	4.3(−5)	8.7(−5)	1.0(−5)	1.3(−6)	5.2(−5)	4.1(−7)	1.3(−5)
$I(110°)/I(70°)$	7.7(−1)	4.9(−2)	4.7(−2)	4.4(−2)	6.9(−2)	2.1(−2)	4.5(−4)	4.4(0)	6.0(−5)	2.9(−2)
$I(150°)/I(30°)$	1.2(−1)	1.5(−4)	1.3(−4)	1.1(−4)	2.9(−4)	3.7(−5)	2.9(−5)	4.3(−4)	1.8(−5)	6.5(−5)

[a] Distorted wave plus exchange.
[b] Abbreviations are defined in Tables VII and VIII.

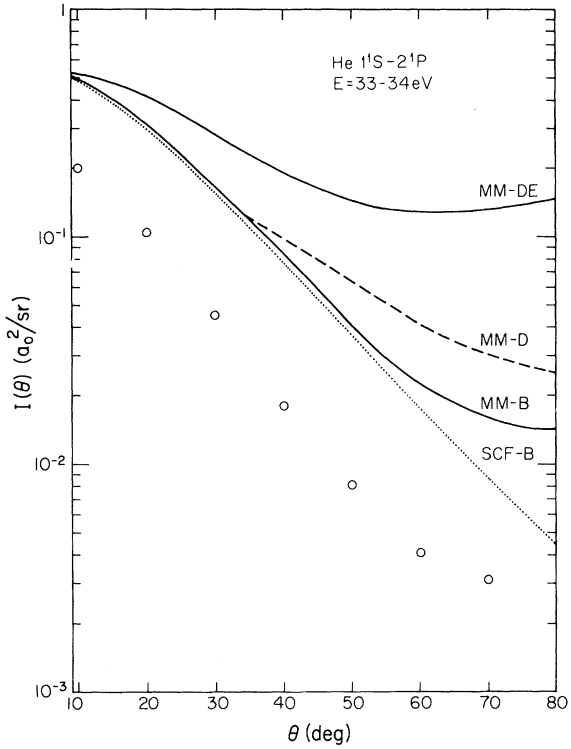

FIG. 16. Comparison of experimental differential cross section (circles) and Born approximation calculation using SCF set of generalized oscillator strengths (dotted curve) at $E = 34$ eV with calculations of Massey and Mohr at $E = 33$ eV (full and dashed curves: B-Born approximation; D-distorted wave calculation; DE-distorted wave plus exchange calculations). The experimental differential cross section is normalized to the experimental integral cross section of Jobe and St. John (see Sec. II C) and the Massey-Mohr differential cross sections are normalized as explained in Sec. V B 1.

the region where the shapes agree (about $\theta = 20°$ for the data in this paper) and determining the angle at which they deviate by 50%. Equation (39) can then be used to determine an upper limit $q_{\max}{}^{B}$ for the momentum transfer for which the Born or BOR approximation is approximately valid at this energy. (Other criteria for choosing $q_{\max}{}^{B}$ that we have tried yield qualitatively the same results and conclusions.) Figure 17 shows a plot of $q_{\max}{}^{B}$ versus $(E - \Delta E)$. The figure also includes lower limits for $q_{\max}{}^{B}$ in the range 100 – 400 eV determined from the data of Ref. 7 and at 511 eV determined from the data of Ref. 4. Lines are drawn for $q_{\min}$ and $q_{\max}$, which define the physical region of q for any energy. Because theory and experiment disagree so much at 26.5 eV, we can only determine an upper limit on $q_{\max}{}^{B}$ there. But this does indicate that if we draw a curve for $q_{\max}{}^{B}(E)$ it will intersect $q_{\min}(E)$ between 26.5 and 34 eV. Although more large scat-

TABLE X. Integral cross sections including exchange for excitation of the 2^1P state of helium. (Number in parentheses is power of 10 by which value given is to be multiplied.

Calculation	$E = 21.6$ eV	$E = 22.0$ eV
BCO-c.c. [a]	1.82(−2)	2.41(−2)
KI -B [b]	9.29(−2)	1.33(−1)
O	2.59(−2)	4.09(−2)
BOR	1.83(−1)	2.53(−1)
OP	6.37(1)	1.94(1)
BORP	5.29(−2)	7.73(−2)
BORB. I	3.24(−2)	4.98(−2)
BTKF	1.07(−1)	1.51(−1)
BTVPS	2.60(−2)	4.10(−2)
BKK-B	1.03(−1)	1.47(−1)
BORB. I	3.60(−2)	5.51(−2)
SCF-B	8.62(−2)	1.23(−1)
BORB. I	3.01(−2)	4.60(−2)

[a]Reference 82.

[b]The first abbreviation indicates the set of generalized oscillator strengths (see Appendix), and the second indicates the method. The abbreviations are: B Born approximation; O and OP Ochkur approximation (prior and post); BOR, BORP, and BORB. I Born-Ochkur-Rudge approximation (prior, post, and symmetrized); BTKF Born-transferred Kang-Foland approximations; BTYPS Born-transferred-Vainshtein-Presnyakov-Sobelman approximation.

tering-angle experiments will be required to completely delineate the curve, the plot does indicate that it is a smooth function. Then, (q, E) are a better set of variables than (θ, E) for expressing the range of validity of the first Born-approximation assumptions. For the intermediate energy range of most interest in this paper, $q_{\max}^{B}$ is about $1.4-1.8\,a_0^{-1}$. The discrepancies in other ranges are not unexpected. It is expected on physical grounds that first-order theories are not valid near threshold because distortion is not adequately represented in these models. Similarly, even at high energies, the collisions resulting in large momentum transfer involve large perturbations. Hence, distortion is again important and first-order models are not expected to be valid.

VI. EXCHANGE CROSS SECTIONS AND FURTHER DISCUSSION OF EXCHANGE

The exchange scattering contribution to electron-atom scattering provides a sensitive test of theories of rearrangement collisions.[23, 26] In our case the exchange cross section is computed by retaining only the second term (i.e., $|G|^2$) in Eq. (12). Thus, the exchange cross section is the same in the prior OR, post OR and symmetrized OR approximations. Also, the exchange differential cross sections in the prior and post Ochkur and prior, post, and symmetrized OR approximations have exactly the same shape. Some typical exchange cross sections for excitation of the 2^1P state of He are shown in Figs. 18 and 19. At lower energies all the exchange cross sections calculated here, except the transferred KF one, are peaked off zero degrees. Above 50 eV, the transferred KF differential cross section also is peaked off zero degrees. Table XI gives the positions of these peaks at some of the higher energies. The behavior of the peaks is quite similar to the behavior of the peaks for the Ochkur or OR approximation for the $1s$-$2s$ excitation in hydrogen.[26]

Joachain and Mittleman[23] distinguished two problems in calculating electron-atom exchange scattering: the dynamical problem and the bound state problem; Joachain and Mittleman used poor bound-state wave functions.[23] Our results are based on very accurate wave functions, so that we have eliminated much of the bound-state problem. This leaves the dynamical problem, and the differences among the exchange cross sections calculated here can be attributed to differences in the theories. Since the dynamical problem is far from solved,

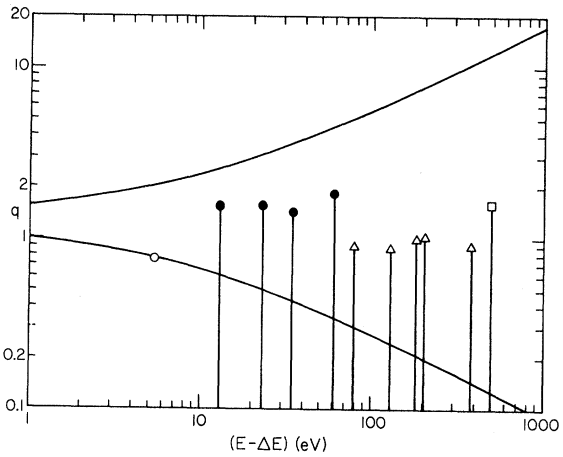

FIG. 17. The region ℬ in which the Born approximation predicts the shape, i.e., angle dependence, of the differential cross section, approximately correctly for excitation of the 2^1P state of helium. The ordinate is momentum transfer and the abscissa is energy above threshold (21.216 eV). The two curved lines bound the physical region [$0° \leq \theta \leq 180°$; cf. Eq. (39)]. The filled circles are $q_{\max}^{B}$, i.e., they are on the upper boundary of ℬ. The open circle is on or above the boundary of ℬ. These circles are derived from the present experiments and calculations. The triangles and square lie below the boundary of ℬ. They are derived from the experiments of Vriens, Simpson, and Mielczarek (Ref. 7) and Silverman and Lassettre (Ref. 4), respectively, and the present calculations. Thus, the vertical lines are wholly in the region ℬ.

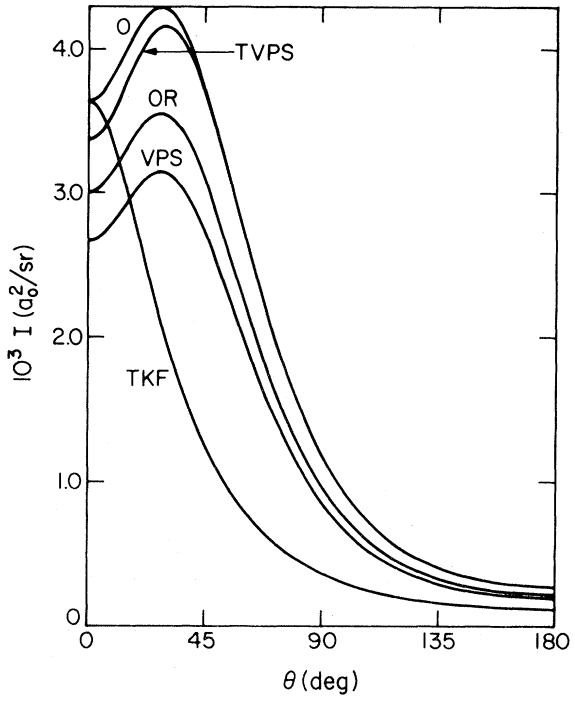

FIG. 18. Exchange differential cross section for excitation of 2^1P state of helium as computed from the KI set of generalized oscillator strengths. $E=34$ eV. The curve labels are: O-prior Ochkur approximation; OR-prior Ochkur-Rudge approximation; TVPS-transferred Vainshtein-Presnyakov-Sobelman approximation; TKF-transferred Kang-Foland approximation; VPS-method of Vainshtein, Presnyakov, and Sobelman. The VPS curve is from Ref. 72.

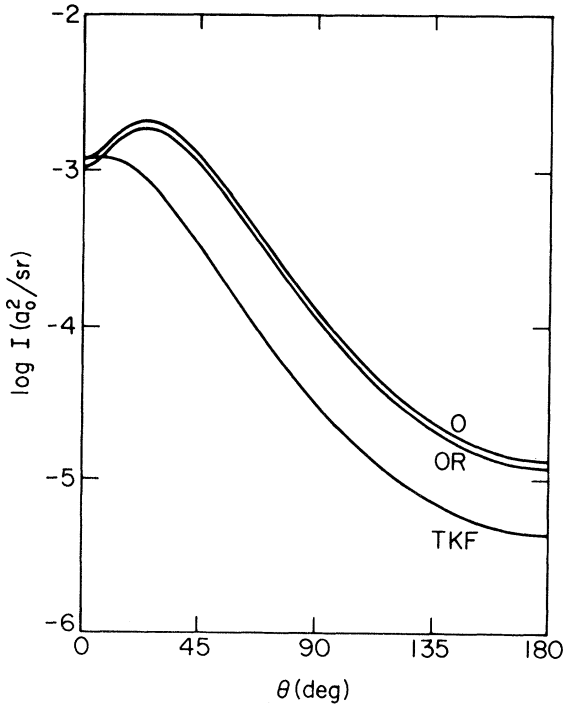

FIG. 19. Exchange differential cross section for excitation of 2^1P state of helium as computed from the KI set of generalized oscillator strengths; $E=55.5$ eV. The curve labels are: O-prior Ochkur approximation; OR-prior Ochkur-Rudge approximation; TKF-transferred Kang-Foland approximation. The transferred VPS approximation is not shown because it is very close to the O curve from 25° to 180° and is between the O and OR at 0°. The post Ochkur approximation exchange DCS is 2.6 times higher than the O at this energy. (The logarithm is to the base 10.)

Table XII gives calculated integral exchange cross sections that may be compared with each other and with future attempts to treat this important problem.

Because the Ochkur and OR theories for the differential cross section have been shown to be in disagreement with experiment [7, 10] and more accurate theory[26] for the exchange scattering in two previous cases (H 1s-2s and He triplet excitation), where they predicted differential cross sections with peaks off zero degrees, [84] it is an interesting question whether a discrepancy in the exchange scattering is at least partially responsible for some of the present disagreement. It would be very interesting to calculate the exchange-scattering differential cross section in the BO approximation[35] or a first-order-exchangelike approximation (such as the first-order theory of Bates, Bassel, Gerjuoy and Mittleman[23, 26, 85]) for comparison with the present results. Calculations in the first-order-exchangelike approximations for helium have so far been limited to singlet-triplet transitions.

Bates, Fundaminsky, Leech, and Massey[79] reported a BO calculation of the integral cross-sec-

TABLE XI. Positions of the peaks (scattered angle θ in degrees) in the exchange differential cross section for excitation of the 2^1P state of helium.

E(eV)	OR [a]	TVPS [b]	TKF [c]
75	21	21	12
100	18	18	12
200	13	13	11
300	10	11	9
400	9	9	8
500	8	8	7
700	7	7	6
1000	6	6	5
4000	3	3	3

[a] Prior Ochkur-Rudge approximation.

[b] Transferred Vainshtein-Presnyakov-Sobelman approximation.

[c] Transferred Kang-Foland approximation.

TABLE XII. Integral exchange cross sections (a_0^2) computed from Kim-Inokuti set of $\phi_{0n}(q)$. (Numbers in parentheses are powers of 10 by which given numbers are to be multiplied.)

E (eV)	O [a]	OP [b]	OR [c]	TKF [d]
22.00	2.87(−2)	2.27(1)	2.16(−2)	2.13(−2)
25.00	3.82(−2)	1.67(0)	2.97(−2)	2.05(−2)
27.21	3.45(−2)	7.11(−1)	2.73(−2)	1.63(−2)
30.61	2.73(−2)	2.90(−1)	2.22(−2)	1.14(−2)
40.00	1.38(−2)	6.27(−2)	1.78(−2)	4.90(−3)
54.40	5.77(−3)	1.55(−2)	5.12(−3)	1.94(−3)
81.63	1.75(−3)	3.19(−3)	1.61(−3)	6.14(−4)
100.00	9.56(−4)	1.54(−3)	8.95(−4)	3.52(−4)
122.44	5.22(−4)	7.64(−4)	4.95(−4)	2.03(−4)
175.00	1.79(−4)	2.32(−4)	1.73(−4)	7.78(−5)
272.10	4.77(−5)	5.61(−5)	4.66(−5)	2.38(−5)
400.00	1.50(−5)	1.68(−5)	1.48(−5)	8.37(−6)
700.00	2.81(−6)	2.94(−6)	2.78(−6)	1.80(−6)
1000.00	9.62(−7)	1.00(−6)	9.56(−7)	6.70(−7)
4000.00	1.50(−8)	1.52(−8)	1.50(−8)	1.29(−8)

[a] Prior Ochkur approximation.
[b] Post Ochkur approximation.
[c] Prior Ochkur-Rudge approximation.
[d] Transferred Kang-Foland approximation.

tion curve for excitation of the 2^1P state of helium. This predicted an even steeper initial rise and a higher peak at lower energy than the Born approximation, thus making the comparison with experiment even worse. The total cross section might be improved if some unitarization[26, 86] were performed in the BO exchange amplitude. In the BO calculations the cross sections are much worse (larger) for the post form than the prior form,[79] which is just the opposite of the present situation with the BOR and Ochkur approximations (except for the post Ochkur approximation near threshold). In the BO approximation, the post-prior discrepancy is a measure of the lack of quality of the wave function.[87] However, the prior and post BOR approximations do not become identical even for the exact bound-state wave functions. Thus, in this case the post-prior discrepancy is a measure of the scattering approximation itself. We note that Altshuler[88] has discerned a preference, on formal grounds, for the prior formulation of the exchange amplitude. From the point of view of our numerical calculations, the BOR approximation is in better agreement than the BORP approximation with the shape of the experimental DCS. Perhaps the better agreement of the latter with the experimental integral cross section is fortuitous. Or perhaps we should not trust the conclusions about their relative merits because neither the prior OR nor the post OR exchange amplitude has been shown to have a phase compatible with the Born direct amplitude.[45] Using detailed balance as a criterion for the phase of the exchange amplitude leads to the BORB. I approximation, but this leads to a nonphysical zero in the differential cross section. The problem of finding an appropriate exchange amplitude remains unsolved.

VII. SUMMARY

We have presented five experimental differential cross sections for excitation of the 2^1P state of helium in the range $10° \leq \theta \leq 80°$, 26.5 eV $\leq E \leq$ 81.6 eV. These were found to be in qualitative agreement with our Born-Ochkur-like calculations only in the range $10° \leq \theta \leq 40°$, 34 eV $\leq E \leq$ 81.6 eV. All of the calculations reported here give differential cross sections which are too small at larger scattering angles, evidently due to neglect of distortion. We have examined the predictions of the first-order theory for both integral and differential, total and exchange cross sections for this transition. Of the three newest calculational methods, the BORB. I approximation and the BTVPS approximation were found to have some similarities to the prior Ochkur method, which makes them useful for integral cross sections but the BTKF approximation may have fewer disadvantages (along with the prior BOR approximation) for large angle scattering.

The BOR approximation in the post and symmetrized forms and the Ochkur approximation give integral cross sections in better agreement with experiment than the Born approximation. They are an improvement, in this respect, over some other methods of including exchange which greatly overestimate the cross section. The prior form of the BOR approximation gives worse integral cross sections, but gives the angular dependence of the intermediate energy cross section more accurately than any other calculaton. Moreover, it is sufficient to explain all the differential cross-section data available at energies above 82 eV (at these

energies all the data is for small scattering angle).

We have shown that use of good analytic SCF functions for both the ground and excited states yields a generalized oscillator-strength curve different from the one obtained from highly accurate correlated wave functions. Nevertheless, the shape of the $Q(E)$ curve is not affected much and the differential cross sections are qualitatively the same. For any quantitative (i.e., better than about 20%) comparison of differential cross sections, however, the differences are too important to be neglected. This will make it difficult to accurately test the Born approximation for electron-molecule scattering, for which accurate correlated wave functions are generally not available. It will also limit the usefulness of the Born approximation until such wave functions are obtained.

ACKNOWLEDGMENT

We thank Dr. Walter Williams for his help in taking the 81.6-eV experimental data.

APPENDIX: FITS TO GENERALIZED OSCILLATOR STRENGTHS

For all the fits to 1^1S-2^1P generalized oscillator strengths, we took $\alpha = 3.391$ [Eq. (38)]. The other parameters are given in Table XIII.

TABLE XIII. Analytic fit of theoretical generalized oscillator strengths.

Fit	1	2	3
	KI	KKB	SCF
ϕ_{0n} (0)	0.2759	0.2882	0.242
C_1	0.456266	0.686236	0.739273
C_2	0.414351	0.334447	−1.81866
C_3	−1.74889	−0.312246	11.3724
C_4	6.87112	−0.797749	−21.5758
C_5	−10.0300		15.0046
C_6	4.99172		

The first fit was obtained from 51 values of $\phi_{0n}(q)$ in the range $q = 0.224$–4.47 calculated by Kim and Inokuti.[19] The fit is good to better than 0.1% and has $N = 6$.

The second fit was obtained from 20 values of $\phi_{0n}(q)$ in the range $q = 0.1 - 3.0$ calculated in the length formulation by Kennedy, Kingston, and Bell.[17,18] The fit is good to about 0.1% and has $N = 4$.

The third fit was obtained from 134 values of $\phi_{0n}(q)$ in the range $q = 0.212$–6.54 calculated by us from SCF wave functions. It is good to about 1% and has $N = 5$. The actual optical oscillator strength $\phi_{0n}(0)$ yielded by this calculation was 0.24234. Further, in the notation of Ref. 19, these wave functions give $Z_n^{(1)} = 0.404864$.

*Work supported in part by the U. S. Atomic Energy Commission, Report Code No. CALT-767P4-42. Contribution No. 3870 from the Arthur Amos Noyes Laboratory of Chemical Physics, California Institute of Technology.

†Work supported in part by the National Aeronautics and Space Administration under Contract No. NAS-7-100.

‡NATO Postdoctoral Fellow, 1967-1968. Present address: Department of Physics, University of Colorado, Boulder, Colo. 80302.

[1]J. K. Rice, D. G. Truhlar, D. C. Cartwright, and S. Trajmar (to be published).

[2]J. D. Jobe and R. M. St. John, Phys. Rev. 164, 117 (1967).

[3]E. N. Lassettre, M. E. Krasnow, and S. M. Silverman, J. Chem. Phys. 40, 1242 (1964).

[4]S. M. Silverman and E. N. Lassettre, J. Chem. Phys. 40, 1265 (1964).

[5]J. A. Simpson, M. G. Menendez, and S. R. Mielczarek, Phys. Rev. 150, 76 (1966).

[6]E. N. Lassettre, A. Skerbele, and V. D. Meyer, J. Chem. Phys. 45, 3214 (1966).

[7]L. Vriens, J. A. Simpson, and S. R. Mielczarek, Phys. Rev. 165, 7 (1968).

[8]H. Ehrhardt, L. Langhans, and F. Linder, Z. Physik 214, 179 (1968); D. Andrick, H. Ehrhardt, and M. Eyb, Z. Physik 214, 388 (1968).

[9]G. E. Chamberlain, J. A. Simpson, S. R. Mielczarek, and C. E. Kuyatt, J. Chem. Phys. 47, 4266 (1967).

[10]A. Kuppermann, J. K. Rice, and S. Trajmar, J. Phys. Chem. 72, 3894 (1968).

[11]S. Trajmar, D. C. Cartwright, J. K. Rice, R. T. Brinkmann, and A. Kuppermann, J. Chem. Phys. 49, 5464 (1968).

[12]Many additional references are given as footnotes 1–9 of Ref. 11 and as footnotes 126–149 of S. P. McGlynn, T. Azumi, and M. Kinoshita, Molecular Spectroscopy of the Triplet State (Prentice-Hall, Inc., Englewood Cliffs, New Jersey, 1969), Chap. 2.

[13]M. Born, Z. Physik 38, 803 (1926).

[14]H. Bethe, Ann. Physik 5, 325 (1930).

[15]V. I. Ochkur, Zh. Eksperim. i Teor. Fiz. 45, 734 (1963) [English transl.: Soviet Phys. – JETP 18, 503 (1964)].

[16]R. A. Bonham, J. Chem. Phys. 36, 3260 (1962).

[17]D. J. Kennedy and A. E. Kingston, J. Phys. B1, 195 (1968).

[18]K. L. Bell, D. J. Kennedy, and A. E. Kingston, J. Phys. B1, 204 (1968).

[19]Y.-K. Kim and M. Inokuti, Phys. Rev. 175, 176 (1968). The authors are grateful for preprints of this paper.

[20]A representative sampling of this work, especially as applied to electron-atom collisions, may be found in References 7, 17–19, and 21–29.

[21]A. R. Holt and B. L. Moiseiwitsch, Advan. At. Mol. Phys. 4, 143 (1968).

[22]L. Vainshtein, in The Physics of Electronic and Atomic Collisions: Invited Papers from the Fifth Conference, edited by L. M. Branscomb (University of Colorado Press, Boulder, 1968), p. 122.

[23]C. J. Joachain and M. H. Mittleman, Phys. Rev. 140, A432 (1965); 151, 7 (1966).

[24]S. M. Silverman and E. N. Lassettre, J. Chem. Phys. 44, 2219 (1966).

[25]L. Vriens, C. E. Kuyatt, and S. R. Mielczarek, Phys. Rev. 170, 163 (1968).

[26]D. G. Truhlar, D. C. Cartwright, and A. Kuppermann, Phys. Rev. 175, 113 (1968).

[27]A. Skerbele and E. N. Lassettre, Fifth International Conference on the Physics of Electronic and Atomic Collisions, edited by I. P. Flaks (Nauka Publishing House, Leningrad, 1967), p. 495.

[28]K. L. Bell, D. J. Kennedy, and A. E. Kingston, J. Phys. B1, 322 (1968). Equation (1) of this reference gives the cross section in a_0^2, not πa_0^2.

[29]K. L. Bell and A. E. Kingston, J. Phys. B1, 521 (1968).

[30]R. M. St. John, F. L. Miller, and C. C. Lin, Phys. Rev. 134, A888 (1964).

[31]See H. R. Moustafa Moussa, thesis, University of Leiden, Netherlands, 1967 (unpublished). These results are plotted in Refs. 17–19.

[32]J. K. Rice, A. Kuppermann, and S. Trajmar, J. Chem. Phys. 48, 945 (1968).

[33]In these units $\hbar = m = a_0 = 1$, energy is given in hartrees (1 hartree = 27.210 eV), and integral and differential cross sections are given in a_0^2 and a_0^2/sr, respectively.

[34]L. I. Schiff, Quantum Mechanics (McGraw-Hill Book Co., New York, 1955), 2nd ed., p. 244.

[35]D. R. Bates, A. Fundaminsky, and H. S. W. Massey, Phil. Trans. Roy. Soc. London A243, 93 (1950), pp. 111–112.

[36]For the derivation of (5)–(7) from (4), see, e.g., E. H. S. Burhop, in Quantum Theory. I. Elements, edited by D. R. Bates (Academic Press Inc., New York, 1961), p. 392 f. The 2 in Eq. (6) comes about because helium has 2 electrons [the two terms in the potential in Eq. (4)]. See, also, B. L. Moiseiwitsch and S. J. Smith, Rev. Mod. Phys. 40, 238 (1968), Eqs. (16)–(20).

[37]In this paper, we do not use the velocity or acceleration forms.

[38]J. R. Oppenheimer, Phys. Rev. 32, 361 (1928).

[39]I.-J. Kang and C. K. Choi, Phys. Rev. 171, 123 (1968).

[40]E. H. S. Burhop, Ref. 36, p. 397.

[41]W. F. Miller and R. L. Platzman, Proc. Phys. Soc. (London) 70, 299 (1957); E. N. Lassettre and S. A. Francis, J. Chem. Phys. 40, 1208 (1964); E. N. Lassettre, A. Skerbele, and M. A. Dillon, J. Chem. Phys. 50, 1829 (1969). Lassettre and co-workers sometimes use Eqs. (11) and (12) with $G = 0$ and experimental differential cross sections to define an apparent generalized oscillator strength which is equivalent to the definition used here only when the Born approximation is valid.

[42]See also S. P. Khare, Phys. Rev. 149, 33 (1966).

[43]M. R. H. Rudge, Proc. Phys. Soc. (London) 85, 607 (1965); 86, 763 (1965).

[44]D. S. F. Crothers, Proc. Phys. Soc. (London) 87, 1003 (1966).

[45]O. Bely, Nuovo Cimento 49, 66 (1967).

[46]D. J. T. Morrison and M. R. H. Rudge, Proc. Phys. Soc. (London) 91, 565 (1967). The notation f and g and sign convention of this article and Ref. 45 are the same as those in the present article and are standard. In Ref. 26 we used the negative-sign convention to make comparison with the close-coupling calculations less cumbersome.

[47]The symmetrized Born-Ochkur-Rudge approximation has previously been applied to the $1s$-$2s$ excitation of the hydrogen atom [D. G. Truhlar (unpublished)]. In that case it predicted integral cross sections which were smaller and in better agreement with experiment than the prior Ochkur and prior Born-Ochkur-Rudge integral cross sections, but were larger than the theoretical cross sections in D. J. T. Morrison and M. R. H. Rudge, Proc. Phys. Soc. (London) 89, 45 (1966).

[48]I.-J. Kang and W. D. Foland, Phys. Rev. 164, 122 (1967). Our definitions of α, β, γ, and χ are equivalent to those of Kang and Foland.

[49]They are evaluated using formulas 13.1.2, 15.1.1, and 15.3.8 in Handbook of Mathematical Functions, edited by M. Abramowitz and I. A. Stegun (U. S. Department of Commerce, National Bureau of Standards, Washington, D. C., 1964), Appl. Math. Ser. 55, Chap. 13, p. 503, formula 13.6.1. The necessary γ functions were evaluated using formula 6.1.34 of this reference.

[50]L. Vainshtein, L. Presnyakov, and I. Sobelman, Zh. Eksperim. i Teor. Fiz. 45, 2015 (1963) [English transl.: Soviet Phys. – JETP 18, 1383 (1964)].

[51]L. Vainshtein, V. Opykhtin, and L. Presnyakov, Zh. Eksperim. i Teor. Fiz. 47, 2306 (1964) [English transl.: Soviet Phys. – JETP 20, 1542 (1965)].

[52]L. Presnyakov, I. Sobelman, and L. Vainshtein, in Atomic Collision Processes, edited by M. R. C. McDowell (North-Holland Publishing Co., Amsterdam, 1964), p. 243.

[53]A review is given by B. L. Moiseiwitsch and S. J. Smith, Rev. Mod. Phys. 40, 238 (1968).

[54]M. R. C. McDowell, in Fourth International Conference on the Physics of Electronic and Atomic Collisions (Science Bookcrafters, Hudson-on-Hastings, New York, 1965), p. 20.

[55]B. L. Moiseiwitsch and S. J. Smith, Rev. Mod. Phys. 40, 253f. (1968).

[56]L. Presnyakov, I. Sobelman, and L. Vainshtein, Proc. Phys. Soc. (London) 89, 511 (1966).

[57]D. S. F. Crothers, Proc. Phys. Soc. (London) 91, 855 (1967).

[58]A. W. Weiss, J. Res. Natl. Bur. Std. (U.S.) 71A, 163 (1967).

[59]D. C. Cartwright and W. A. Goddard III (unpublished).

[60]R. P. Hurst, Acta Cryst. 13, 634 (1960); W. Kolos and K. Pecul, Ann. Phys. (N.Y.) 16, 203 (1961).

[61]See also S. Huzinaga, Progr. Theroet. Phys. 23, 562 (1960); D. C. Cartwright and A. Kuppermann, Phys. Rev. 163, 86 (1967).

[62]See W. A. Goddard III, J. Chem. Phys. 48, 1008 (1968).

[63]L. Brillouin, J. Phys. Radium 7, 373 (1932); C. Moller and M. S. Plesset, Phys. Rev. 46, 618 (1934); W. A. Goddard III, J. Chem. Phys. 48, 5337 (1968).

[64]E. N. Lassettre, J. Chem. Phys. 43, 4479 (1965).

[65]L. Vriens, Phys. Rev. 160, 100 (1967).

[66]S. Altshuler, Phys. Rev. 87, 992 (1952).

[67]R. M. St. John, F. L. Miller, and C. C. Lin, Phys. Rev. 134, A888 (1964).

[68]B. L. Moiseiwitsch and S. J. Smith, Rev. Mod. Phys. 40, 296 (1968).

[69]I. P. Zapesochnyi and P. V. Feltsan, Opt. Spectry. (USSR) 18, 514 (1965).

[70](a) I. P. Zapesochnyi, Astron. Zh. 43, 954 (1966) [English transl.: Soviet Astron. – AJ 10, 766 (1967)]. (b) I. P. Zapesochnyi, Dokl. Akad. Nauk SSSR 171, 559 (1966) [English transl.: Soviet Phys. – Doklady 11, 961 (1967)].

[71]A. T. Jusick, C. E. Watson, L. R. Peterson, and A. E. S. Green, J. Geophys. Res. 72, 3943 (1967).

[72]This same type dip and zero in the large angle DCS is also present and is very similar in the untransferred VPS approximation [D. G. Truhlar (unpublished)]. Note that this zero is not related to the singularity pointed out by McDowell (Ref. 54) and Crothers (Ref. 57) in altered versions of the VPS approximation.

[73]W. Rothenstein, Proc. Phys. Soc. (London) A67, 673 (1954). Rothenstein's results are compared with first-Born-approximation calculations in J. van den Bos, Technical Report Amolf 67/487, F.O.M. No. 24274 (F.O.M.-Instituut voor Atoom-en Molecuulfysica, Amsterdam, 1967).

[74]B. L. Moiseiwitsch and S. J. Smith, Rev. Mod. Phys. 40, 245 (1968).

[75]L. A. Vainshtein and G. G. Dolgov, Opt. i Spektroskopiya 7, (1959) [English transl.: Opt. Spectry. (USSR) 7, 1 (1959)].

[76]H. S. W. Massey and C. B. O. Mohr, Proc. Roy. Soc. (London) A132, 605 (1931). There appears to be an error in the ordinate for the upper right plot in Fig. 2.

[77]H. S. W. Massey and C. B. O. Mohr, Proc. Roy. Soc. (London) A139, 187 (1933).

[78]A. Fundaminsky, thesis, 1949, published in Ref. 79 and in Ref. 53.

[79]D. R. Bates, A. Fundaminsky, J. W. Leech, and H. S. W. Massey, Phil. Trans. Roy. Soc. London A243, 117 (1950).

[80]B. L. Moiseiwitsch and S. J. Smith, Rev. Mod. Phys. 40, 247 (1968); 40, 260–261 (1968).

[81]Massey and Mohr neglected exchange during the actual determination of their distorted waves. It is now known (conversely to the effect mentioned in the text) that the exchange has an important effect on the distortion, especially at energies within 10 eV of threshold. See G. Erskine and H. S. W. Massey, Proc. Roy. Soc. (London) A212, 521 (1952); H. S. W. Massey and C. B. O. Mohr, *ibid.* A65, 845 (1952); H. S. W. Massey and B. L. Moiseiwitsch, *ibid.* A227, 38 (1954); and more recent close coupling calculations with and without exchange.

[82]P. G. Burke, J. W. Cooper, and S. Ormonde, Phys. Rev. Letters 17, 345 (1966).

[83]Some discussion of the possibility that the Born approximation is more valid at high and low momentum transfers than intermediate ones is given in E. N. Lassettre, A. Skerbele, and M. A. Dillon, J. Chem. Phys. 50, 1829 (1969). We will only discuss the lack of validity which arises when q becomes too large for the low q domain.

[84]However, there is better agreement in the case of hydrogen molecule (Ref. 11). We also expect better agreement for ethylene.

[85]K. L. Bell, H. Eissa, and B. L. Moisiewitsch, Proc. Phys. Soc. (London) 88, 57 (1966).

[86]A. Y. Abul-Magd and M. H. Simbel, Z. Physik 215, 121 (1968).

[87]N. F. Mott and H. S. W. Massey, The Theory of Atomic Collisions (Clarendon Press, Oxford, England, 1965), pp. 421–422, 3rd ed.

[88]S. Altshuler, Phys. Rev. 91, 1167 (1953).